

Kendon EJ, Blenkinsop S, Fowler HJ.

[When will we detect changes in short-duration precipitation extremes?](#).

*Journal of Climate* 2018. In Press.

**Copyright:**

Permission to place a copy of this work on this server has been provided by the AMS. The AMS does not guarantee that the copy provided here is an accurate copy of the published work.

**Date deposited:**

23/01/2018

1 **When will we detect changes in short-duration precipitation extremes?**

2

3

4

Elizabeth J. Kendon\*

5

Met Office Hadley Centre, Exeter, UK

6

7

Stephen Blenkinsop, Hayley J. Fowler

8

School of Engineering, Newcastle University, UK

9

10 \*Corresponding author address: Elizabeth Kendon (nee Kennett), Met Office Hadley Centre,

11 Fitzroy Road, Exeter, EX1 3PB, UK.

12 Email: [elizabeth.kendon@metoffice.gov.uk](mailto:elizabeth.kendon@metoffice.gov.uk)

## 13 **Abstract**

14 The question of when we may be able to detect the influence of climate change on UK rainfall  
15 extremes is important from a planning perspective, providing a timescale for necessary climate  
16 change adaptation measures. Short-duration intense rainfall is responsible for flash flooding,  
17 and several studies have suggested an amplified response to warming for rainfall extremes on  
18 hourly and sub-hourly timescales. However, there are very few studies examining the detection  
19 of changes in sub-daily rainfall. This is due to the high cost of very high-resolution (kilometre-  
20 scale) climate models needed to capture hourly rainfall extremes, and to a lack of sufficiently  
21 long high-quality sub-daily observational records. Results here using output from a 1.5km  
22 climate model over the southern UK indicate that changes in 10-minute and hourly  
23 precipitation emerge before changes in daily precipitation. In particular, model results suggest  
24 detection times for short-duration rainfall intensity in the 2040s in winter and 2080s in summer,  
25 which are respectively 5-10 years and decades earlier than for daily extremes. Results from a  
26 new quality-controlled observational dataset of hourly rainfall over the UK do not show a  
27 similar difference between daily and hourly trends. Natural variability appears to dominate  
28 current observed trends (including an increase in the intensity of heavy summer rainfall over  
29 the last 30 years), with some suggestion of larger daily than hourly trends for recent decades.  
30 The expectation of the reverse, namely larger trends for short-duration rainfall, as the signature  
31 of underlying climate change has potentially important implications for detection and  
32 attribution studies.

## 33 **1. Introduction**

34 Recent UK floods (for example, caused by Storm Angus across the country in November 2016,  
35 in the north of the UK in December 2015 and in Somerset in January 2014) have reinforced  
36 the need for the UK to gain a better understanding of how its exposure to flooding may change  
37 in the future with global warming. This is vital so that appropriate levels of resilience and  
38 protection can be delivered through river and land management and investment in flood  
39 defences (Cabinet Office & DEFRA, 2016). Short-duration intense rainfall is responsible for  
40 flash flooding, important in small, steep catchments and urban areas. Precipitation data at sub-  
41 daily scales (down to a few minutes) and spatial scales of 1-10 km<sup>2</sup> are needed for urban  
42 drainage design (Arnbjerg-Nielsen et al., 2013) and hence an understanding of changes in  
43 precipitation at these scales is important so urban planners can start accounting for the effects  
44 of future climate change. Notable UK examples of this type of extreme event were the floods  
45 in Boscastle in August 2004 and Newcastle-upon-Tyne in June 2012 (Archer and Fowler,  
46 2015), causing extensive damage and major disruption.

47

48 In the context of climate change, with increasing temperature the atmosphere is able to hold  
49 more moisture, and this is expected to lead to future increases in heavy rainfall intensity  
50 (Trenberth et al., 2003). Further, it has recently been argued that observational evidence of the  
51 intensification of extreme rainfall is beginning to show consistency with model studies (Fischer  
52 & Knutti, 2016). The Clausius-Clapeyron relation (hereafter referred to as ‘CC’) suggests that  
53 if relative humidity remains constant, atmospheric humidity will increase at a rate that follows  
54 the saturation vapour pressure dependency on temperature according to the CC relation – a  
55 rate of ~7% per °C of surface warming (e.g. Allen and Ingram, 2002; Pall et al., 2007). This  
56 sets a scale for change in precipitation extremes (Trenberth et al., 2003). Several studies have  
57 provided observational evidence of a super-CC (2x CC) relationship for hourly (e.g., Lenderink

58 & van Meijgaard, 2008, 2010, Mishra et al., 2012) and sub-hourly (e.g. Loriaux et al., 2013)  
59 extremes which might suggest an amplified response to warming on these timescales. Such  
60 super-CC scaling seems to be a property of convective precipitation (Berg et al., 2013), and  
61 may be explained by latent heat released within storms invigorating vertical motion, leading to  
62 a greater increase in rainfall intensity. The dependency of extreme UK hourly rainfall on  
63 temperature has been demonstrated to be consistent with CC scaling in observations  
64 (Blenkinsop et al., 2015) and a high resolution, convection-permitting climate model (Chan et  
65 al., 2016a) but no evidence has been identified of super-CC scaling, including for simulated  
66 10-minute extremes (Chan et al., 2016b).

67

68 Relatively coarse resolution projections (25km) provided by UKCP09 (Murphy et al., 2009)  
69 suggest changes in the wettest day of winter (~99th percentile of daily precipitation) range from  
70 zero in parts of Scotland to +25% in parts of England (central estimate, 2080s, medium  
71 emissions) whilst changes in the wettest day in summer range from -12% in parts of southern  
72 England to +12% in parts of Scotland. Summer changes are however subject to high levels of  
73 uncertainty associated with the parameterization of convection in these models. Typically,  
74 projected changes in sub-daily extremes have been assessed using statistical methods to  
75 disaggregate daily precipitation from regional climate models. Darch et al. (2016) used a  
76 weather generator to provide illustrative results for 10 UK sites to show a projected increase in  
77 the intensity of short-duration events in winter but a reduction in summer. Again, however,  
78 these are associated with high uncertainty due to the underlying climate model resolution and  
79 the fact that they do not use climate change information at the sub-daily scale. This is being  
80 addressed by the new generation of very high resolution, convection-permitting models  
81 (CPMs), which explicitly represent convection without the need for a parameterization scheme.  
82 These models are able to more realistically represent convection, and to capture hourly rainfall

83 characteristics including extremes, unlike traditional coarser resolution climate models  
84 (Kendon et al., 2012, Chan et al., 2014b). The first CPM climate change simulations for the  
85 southern UK project an increased intensity of extreme hourly rainfall in summer and almost a  
86 5-fold increase in events above 30mm/h (a critical accumulation threshold used by the Flood  
87 Forecasting Centre to indicate likely flash flooding) (Kendon et al., 2014).

88

89 In common with most other parts of the globe, observed long-term variability and detection of  
90 trends in UK sub-daily rainfall have received little study due to the lack of sufficiently long,  
91 high-quality records (Westra et al., 2014; Hegerl et al., 2015). Faulkner (1999) produced a  
92 relatively simple analysis of changes in UK 1h annual maxima, observing a possible decreasing  
93 trend over the 20<sup>th</sup> century but noted that this was potentially subject to inhomogeneities arising  
94 from changes in rain gauge type and temporal variations in the observing network. Studies of  
95 observed changes in sub-daily rainfall have tended to focus on relatively small regions (with  
96 exceptions for the US (Barbero et al., 2017) and Australia (Westra & Sisson, 2011) and show  
97 inconsistency in their changes although generally suggest an increase in intensity (Westra et  
98 al., 2014). Historical trends in UK daily rainfall have been relatively extensively studied  
99 however, identifying more intense winter rainfall since the 1960s (Osborn et al., 2000; Osborn  
100 & Hulme, 2002; Maraun et al., 2008) with some evidence of a longer term trend (Osborn et al.,  
101 2000; Simpson & Jones, 2014). The contribution to winter rainfall from heavy precipitation  
102 events has also increased (Jenkins et al, 2008) whilst Jones et al. (2013) identify increases in  
103 seasonal maxima and estimated return frequencies in winter. In contrast, summer rainfall  
104 events have shown little change or declined in intensity, whilst longer duration events (multi-  
105 day) have increased (Fowler & Kilsby, 2003a,b; Jones et al., 2013). Simpson & Jones (2014)  
106 note that trends in mean and extreme summer daily precipitation for regional UK precipitation  
107 series (1931-2011) have been mostly negative, whilst Jones et al. (2013) identify spatially

108 varying changes in the median summer maxima. Although for some regions these events  
109 appear to be increasing, in general summer rainfall events have declined in intensity. A recent  
110 study (Brown, 2017) has found that these previously reported trends in UK daily rainfall  
111 extremes, however, may be due at least in part to natural variability. In particular, the North  
112 Atlantic Oscillation (NAO) explains much of the trend in winter extreme rainfall from 1958 to  
113 2012 (with the residual trend after inclusion of NAO much reduced in magnitude and  
114 significance), and any apparent trend in summer extreme rainfall.

115

116 Evidence of human influence on changes in rainfall has been accumulating globally. For  
117 example, Min et al. (2011) showed that human-induced warming has contributed to observed  
118 increases in the intensity of heavy precipitation over large parts of Northern Hemisphere land  
119 areas. However, the attribution of rainfall trends to human influence on local and regional  
120 scales is not yet possible (Sarojini et al., 2016). For some specific extreme events, it is possible  
121 to show that anthropogenic climate change increased the risk of the event e.g. the Autumn 2000  
122 floods in England and Wales (Pall et al., 2011) and the 2014 Southern England winter floods  
123 (Schaller et al., 2016). However, this is not true of many other flooding events, and it is only  
124 with time that we can detect any underlying trend.

125

126 An important measure therefore to inform adaptation planning is detection time, i.e. when  
127 changes in flooding are expected to move outside of what has been experienced in the past due  
128 to natural climate variability. The question of when we may be able to detect the influence of  
129 climate change on UK rainfall is examined here. This is important from a planning perspective,  
130 providing a timescale for necessary climate change adaptation measures. Detection time is also  
131 useful for evaluating climate model projections, as the emergence of the climate change signal  
132 predicted by the model can be tested using observations. Fowler & Wilby (2010) examined UK

133 daily precipitation change from thirteen 50km resolution regional climate model simulations  
134 from the PRUDENCE ensemble, and found changes in the winter 10 year return level emerge  
135 in the 2040s, whilst changes in summer extremes are highly uncertain. A similar study using  
136 the ClimatePrediction.net global climate model ensemble gave similar results (Fowler et al.,  
137 2010).

138

139 In this paper, we examine how detection time varies for UK precipitation accumulated across  
140 a range of time and space scales, including down to 10-minute and kilometre scales, using  
141 output from a very high resolution (convection-permitting) climate model and investigate the  
142 consistency of modelled detection times with observed changes from gauge data in a new,  
143 quality controlled dataset of hourly rainfall for the UK. Convection-permitting models do not  
144 necessarily better represent daily precipitation compared to coarser resolution regional climate  
145 models (Chan et al., 2013), but are needed to provide reliable projections of sub-daily rainfall  
146 and hence an estimate of when we may be able to detect change on these timescales.

147

## 148 **2. Data & Methods**

### 149 *a. Climate model*

150 A very high-resolution (1.5km) climate model spanning the southern UK (including most of  
151 England and Wales) is used here. This was the largest domain possible to allow completion of  
152 decadal length simulations in a reasonable time, and includes regions with different rainfall  
153 characteristics. In particular, it includes southern England, where there is a high proportion of  
154 convective events in summer; London, where the urban environment has a considerable  
155 influence on the local climate; and the mountainous region of Wales, where there is orographic  
156 enhancement of rainfall. The model is a modified version of the non-hydrostatic Met Office  
157 operational UK variable-resolution model (UKV), a configuration of the Met Office Unified



158 Model (UM) and is described in Kendon et al. (2014). For weather forecasting purposes, 1.5km  
159 grid spacing is the finest affordable resolution at which most convection over the UK is  
160 satisfactorily represented on the grid without the need for a convection scheme (Lean et al.,  
161 2008). Thus in this model, the convection parameterization scheme is switched off. 13-year  
162 present- (1996-2009) and future-climate (~2100, RCP8.5 scenario) 1.5-km simulations are  
163 driven by a 12km regional climate model (RCM), which spans Europe and is in turn driven by  
164 a 60km atmosphere-only general circulation model (GCM). The 12km RCM and 60km GCM  
165 both have the UM Global Atmosphere 3.0 configuration (Walters et al., 2011). 10-minute  
166 precipitation has been output for the summer months (June-July-August) only, due to the large  
167 data volume. Chan et al. (2016b) identified an intensification of these 10-minute extremes that  
168 is consistent with that found at hourly timescales, and here we build on these results, examining  
169 whether increases in hourly and 10-minute extremes are detectable before changes in daily  
170 rainfall extremes.

171

172 The 1.5km model is based on the Met Office operational UK weather forecast model, and  
173 extensive testing within numerical weather prediction (NWP) trials indicates that the model  
174 produces realistic convective showers and is able to forecast localised extreme events not  
175 captured at coarser resolutions (Lean et al., 2008). The 1.5km model has also been shown to  
176 realistically capture hourly rainfall in long climate simulations. In particular, Kendon et al.  
177 (2012) showed that the model gives a much better representation of the intensity-duration  
178 characteristics of hourly rainfall, as well as its spatial extent, compared to a coarser resolution  
179 climate model. Kendon et al. (2014) showed the intensity of heavy hourly rainfall and its spatial  
180 pattern across the southern UK is well captured in the 1.5km model in both summer and winter;  
181 whilst Chan et al. (2014b) showed that the model is more realistic in representing hourly  
182 precipitation extremes compared to a 12km climate model. These improvements in the

183 representation of sub-daily rainfall characteristics are also seen in other CPMs for other regions  
 184 (Kendon et al., 2017). There is still a tendency for heavy rainfall to be too intense in the 1.5km  
 185 model, which is a common deficiency in convection-permitting models (Kendon et al., 2017)  
 186 and likely to be a consequence of convection not being fully resolved at kilometre scales. The  
 187 model has not been evaluated at sub-hourly timescales from a climatological perspective, due  
 188 to the lack of UK quality-controlled multi-year sub-hourly observations (Chan et al., 2016b).  
 189 Focussed field campaigns (e.g. DYMECS project) have shown the 1.5km NWP model does  
 190 not adequately represent short-lived storm lifecycles, but results vary with the type of  
 191 convective storms (Stein et al., 2015). We note that 10-minute output corresponds to 12 (50  
 192 second) model time steps, and so is approaching the limit imposed by discretisation.

193

194 Following Fowler & Wilby (2010), we define a detectable increase in a given precipitation  
 195 metric  $D_x$  as the year at which we would reject (at the  $\alpha=0.05$  or 95% significance level) the  
 196 null hypothesis that the metric for year  $x$  ( $\mu_x$ ) and the control period (1996-2009,  $\mu_c$ ) are equal,  
 197 in favour of the alternative hypothesis that  $\mu_x$  is not equal to  $\mu_c$ . Using a two-tailed test (with  
 198 critical Z score of 1.96) this corresponds to:

$$199 \quad |D_x| = \frac{|\mu_x - \mu_c|}{\sqrt{\sigma_f^2 + \sigma_c^2}} \geq 1.96$$

200 where  $\sigma_c^2$  ( $\sigma_f^2$ ) is the variance in the metric for the control (future) period. Assuming a linear  
 201 trend in the metric through time between the present climate simulation (mid-year 2003) and  
 202 the future simulation (mid-year 2103, metric  $\mu_f$ ), we get the following for the earliest  
 203 detection year  $Y_D$ :

$$204 \quad Y_D = 2003 + 196 \frac{\sqrt{\sigma_f^2 + \sigma_c^2}}{|\mu_f - \mu_c|}$$

205 We have used bootstrap resampling to get an estimate of the variance of the metric, due to  
206 natural climate variability, in the control and future periods. For each season, we have  
207 randomly selected 13 years out of the 13-year period, with replacement, such that in the  
208 resampled time series some years occur more than once and other years not at all. By this  
209 method, we are retaining any time correlations on sub-seasonal timescales and only assume  
210 independence between a given season for one year and the next. This resampling is done  
211 identically at each grid point, thus retaining any spatial coherence. The bootstrap resampling  
212 procedure is repeated 100 times, for each of the control and future periods. The precipitation  
213 metric of interest ( $\mu$ ) is then calculated at each grid point, for each of the bootstrap samples.  
214 This allows the detection year  $Y_D$  to be calculated at each grid point, using the variance across  
215 the 100 estimates of  $\mu$  for the control and future periods. We finally calculate the median of  
216 all the detection times across southern UK land points, to give a single central estimate, as  
217 well as the 10<sup>th</sup> and 90<sup>th</sup> percentiles of the spatial varying estimates to give an indication of  
218 uncertainty.

219

220 In this analysis, since we are restricted to single 13-year simulations of the present and future  
221 climate, it is not possible to examine initial condition uncertainty. The method of resampling  
222 only accounts for year-to-year natural variability, with no consideration of multi-decadal  
223 climate variability. The presence of significant multi-decadal variability in the metric could  
224 lead to the actual detection time of the climate change signal being earlier or later than that  
225 estimated above, depending on where the control and future periods fall within this multi-  
226 decadal cycle. We note, however, that given the way the future sea surface temperatures (SSTs)  
227 are configured in the driving GCM, we would expect this effect to be small. In particular, the  
228 future SSTs are configured as a time-invariant delta (given by the multi-year mean SST change  
229 for each month between 1990-2010 and 2090-2110 in HadGEM2-ES) applied onto the present-

230 day time-varying SSTs (as described in Kendon et al., 2014), and human induced warming (of  
231 about 4K globally) is expected to dwarf any influence of natural climate variability in the 20  
232 year mean SST change. Another limitation of the approach here is that it assumes a linear trend  
233 in the metric between the control and future periods. In reality, it is likely that changes will  
234 start more slowly and then accelerate towards the end of the century, following the projected  
235 profile of human-induced warming. This will mean actual detection times are likely to be later  
236 than estimated assuming a simple linear trend. Fowler & Wilby (2010) attempted to model this  
237 effect by applying a pattern scaling approach, assuming regional changes in precipitation will  
238 occur in proportion to the projected change in global mean temperature. In this paper, we just  
239 use the simple linear approach, but note this will not impact the finding of whether changes in  
240 daily or short-duration precipitation emerge first.

241

242 Here we consider three precipitation metrics: i) mean wet day/hour intensity (wet value is  
243  $>0.1$ mm per accumulation period); ii) heavy precipitation intensity, defined as the mean of the  
244 upper 5% of wet values ( $p_{95}$ ); and iii) heavy precipitation, defined as the mean of the upper 1%  
245 of all values ( $p_{99ALL}$ ). The precipitation metrics are calculated for 10-minute, hourly and daily  
246 precipitation accumulations, using the 13 years of data from the control and future simulations  
247 respectively. They are also calculated for the 1.5km precipitation regridded to a range of coarser  
248 spatial scales (5km, 12km and 50km) using area-weighted averaging. All temporal-spatial  
249 averaging is carried out on the raw precipitation time series data before calculation of the  
250 metrics.

251

#### 252 *b. Change detection in observations*

253 To examine whether evidence from historical observations are consistent with the detection  
254 times derived from the model projections, we use a new dataset of hourly precipitation for the

255 UK. It should be noted that this observational analysis uses data across the whole of the UK,  
256 whereas the model data corresponds only to the southern UK. However, we repeated the  
257 analysis with only those gauges within the model domain (Figure 1) and found this did not give  
258 any qualitative difference in the results. The provenance and extensive quality control of the  
259 observational dataset, which is comprised of ~1900 rain gauges are described in Blenkinsop et  
260 al. (2017). They indicate that although the earliest records commence in 1949, most of these  
261 gauges were installed in the 1990s and so the number for which sufficiently long records exist  
262 for trend analysis is limited. The data have been updated for this study to the end of 2014 with  
263 additional quality control procedures, including comparison with neighbouring gauges and  
264 validation against a high quality gridded daily dataset (Lewis et al., 2017). We also compared  
265 annual time series of mean 1h and 24h intensities for all gauges within 25km of each other by  
266 computing the Spearman rank ( $S$ ) correlation coefficient. Such an approach ideally requires a  
267 known, reliable reference gauge to identify potential errors but in this instance most gauges  
268 correlated highly with at least one other gauge. However, one gauge (Milcote, central England)  
269 was excluded from the analysis on the basis of low correlations ( $S < 0.26$  to  $0.4$ ) with three  
270 neighbouring gauges.

271

272 In addition, Blenkinsop et al. (2017) only analysed the climatology of records of ~20y length  
273 and so did not consider potential inhomogeneities that may confound any analysis of change.  
274 We therefore applied a selection of statistical tests to identify breaks in the time series that may  
275 indicate inhomogeneities in the data and in this case enabled the identification of changes in  
276 the measurement resolution of many gauges. The full details of this procedure are provided in  
277 the supporting information.

278

279 For the observational analysis we carry out several approaches to assess the change in  
280 comparison with the model projection:

- 281 i) we calculate the same three precipitation metrics as for the analysis of the model  
282 simulations for the last 13-year period of record (2002-2014) and calculate the  
283 change in each statistic relative to earlier running 13-year periods from the start of  
284 the record up to the period 1989-2001, hereafter referred to as *percentage change*;
- 285 ii) for selected 13-year periods the changes in each metric are then normalised by the  
286 variability in the metric using the same resampling procedure as for the model  
287 analysis, resampling years in the 13-year start and end periods to produce the  
288 statistic  $D_x$ . This allows a direct comparison between the observational and model  
289 analyses. We refer to this approach as *normalised change*;
- 290 iii) in addition to calculating changes in the 13-year statistics, we also calculate trends  
291 in yearly mean intensity and  $p_{95}$  values. This approach provides a less robust  
292 measure of  $p_{95}$  (since this equates to averaging only 5 hourly values in a single  
293 season assuming 5% of hours are wet, and less in the case of daily data) but allows  
294 all the observational data throughout the period of interest to contribute to the trend  
295 estimate and is an approach more typically used for the analysis of changes in a  
296 continuous time series. Trends are calculated using two methods: the longest  
297 available period at each gauge (minimum 30 years) and also using running 30-year  
298 trends calculated from 1950 at 5-year intervals (hereafter referred to as *long* and  
299 *running trends* respectively). The use of running trends allows an assessment of  
300 the sensitivity of any identified trends to the period of the record. Running trend  
301 analysis is a useful descriptive tool for climatic time series (Trottini et al., 2015)  
302 and has been used in a range of climate analyses including attribution studies (e.g.

303 Santer et al., 2014; Hamlington et al., 2013) and model evaluation (Risbey et al.,  
304 2014).

305

306 For the analysis of trends, significant monotonic trends were identified using the Mann Kendall  
307 test (two-tailed, 95% significance level). Trend magnitudes were estimated using the non-  
308 parametric Sen's slope (Theil-Sen estimator). The Theil-Sen estimator of a set of two-  
309 dimensional points  $(x_i, y_i)$  is the median of the slopes  $(y_j - y_i)/(x_j - x_i)$  determined by all pairs of  
310 sample points (Theil, 1950) and was extended (Sen, 1968) for cases where two data points have  
311 the same  $x$ -coordinate (in this instance time is the  $x$  variable). In order to derive trends that are  
312 comparable across accumulation periods we also calculated Sen's relative slope, the slope  
313 joining each pair of observations being divided by the first of the pair before the overall median  
314 is taken (Jassby & Cloern, 2016), providing a normalised trend that allows comparison of series  
315 of different magnitudes and even units. For each period, estimated trend magnitudes for 1h  
316 and 24h accumulations were also compared using a two-tailed Wilcoxon rank-sum test to test  
317 for significant differences in the trend means.

318

319 Gauges were selected for this analysis of change on the basis of their completeness. For  
320 assessments of the change in the 13-year statistics, gauges were only included if they were at  
321 least 85% complete over the period 2002-2014 and at least one other 13-year period. For the  
322 trend analysis we selected those gauges spanning at least 30 years (applying the same criteria  
323 as in Blenkinsop et al. (2017) where each year/season has at least 85% of non-missing data and  
324 a minimum of ~85% of years/seasons must also meet this criteria for use). Further, gauges  
325 meeting these criteria were only included if missing periods did not occur at the beginning  
326 and/or end of a period used for trend estimation (i.e. data present truly reflects the period for  
327 which trends are estimated). In total 123(130) gauges are used in this analysis for DJF(JJA)

328 (Figure 1) but due to missing data the number available at different periods and for different  
329 seasons varies, and fewer gauges were available for trend analysis due to the requirement for  
330 longer, continuous time series. Sub-hourly gauge data from the UK Met Office (provided at a  
331 temporal resolution of 1 min) and tipping bucket rain gauge data from the UK Environment  
332 Agency were also examined but these data did not meet the record length criteria and so  
333 observed change in rainfall on 10-minute timescales could not be assessed.

334

### 335 **c. Modes of variability**

336 To assess the influence of natural variability on observed trends, we examine changes in the  
337 North Atlantic Oscillation (NAO) and the Atlantic Multidecadal Oscillation (AMO), using  
338 the Climatic Research Unit (CRU) NAO index<sup>1</sup> (Jones et al., 1997) and the detrended AMO  
339 index (Enfield et al., 2001) available from NOAA<sup>2</sup>.

340

341 The NAO has long been considered the most important single mode for interpreting climate  
342 variability in the northern hemisphere (Walker, 1924; Hurrell, 1996) including winter  
343 precipitation in Europe (Hurrell, 1995; Hurrell & van Loon, 1997; Trigo et al., 2002; Hoy et  
344 al., 2014) and has been noted to account for many of the observed changes in UK winter  
345 precipitation totals and daily extremes (Simpson & Jones, 2014; Wilby et al., 1997, Brown,  
346 2017). Regional variations in the association between NAO and winter rainfall have been  
347 noted by Wilby et al. (2002).

348

349 Summer atmospheric circulation associated with the NAO identified by Hurrell et al. (2003)  
350 has been noted to have a smaller spatial extent than in winter, and was located further north.  
351 However, the summer NAO (SNAO) has been shown to have the strongest influence on

---

<sup>1</sup> Freely available at: <https://crudata.uea.ac.uk/cru/data/nao/>

<sup>2</sup> Freely available at: <https://www.esrl.noaa.gov/psd/data/timeseries/AMO/>



352 climate over north-western Europe (Linderholm et al., 2009; Hoy et al., 2014). Osborn et al  
353 (2000) showed that ~60% of the variance in annual summer precipitation for regional series  
354 for central, eastern and southern England rainfall can be explained by atmospheric circulation  
355 whilst Folland et al. (2009) identified that the summer (JA) SNAO explains the principal  
356 variations of summer climate over northern Europe, including mean precipitation with very  
357 strong and significant negative correlations of the SNAO index with summer rainfall,  
358 exceeding -0.64 over parts of the British Isles. However, Hoy et al. (2014) suggest that  
359 summer relationships are sensitive to the definition of the SNAO. Simpson & Jones (2014)  
360 did note some significant negative correlations between daily UK summer extreme rainfall  
361 and the SNAO, and consistent with this, Brown (2017) find that positive SNAO reduces the  
362 likelihood of extreme daily rainfall in summer, accounting for much of the variability from  
363 1958 to 2012. In contrast, Wilby et al. (2002) identify positive correlations between the  
364 SNAO and mean summer wet day amount for a cluster of sites across northern Wales and  
365 England. This spatially varying response of the negative phase of the SNAO is also noted by  
366 Hoy et al. (2014).

367

368 The AMO has been noted to be linked to changes in the summer NAO (Folland et al., 2009),  
369 several studies suggesting that 1990s Atlantic warming was a consequence of an acceleration  
370 of the Atlantic Meridional Overturning Circulation (AMOC) linked with the positive phase of  
371 the winter NAO in the 1980s and 1990s (Robson et al., 2012; Lohmann et al., 2009). The  
372 AMO has been identified as an indicator of the importance of the Atlantic Ocean in influencing  
373 European climate, including recent wet summers in northern Europe (Sutton & Dong, 2012).  
374 They indicated that coherent and consistent patterns of precipitation anomalies suggested  
375 changes in atmospheric circulation associated with a warm state of the North Atlantic. We

376 note, however, Brown (2017) finds no influence of the AMO (as an additional covariate to the  
377 NAO) for UK daily extremes.

378

379 In the analysis here, seasonal NAO and AMO indices are calculated as the mean index value  
380 over the corresponding three months, along with 15-year moving averages for comparison  
381 with the trends in  $p_{95}$  observations.

382

### 383 **3. Results**

#### 384 *a. Model detection times*

385 The convection-permitting model (CPM) simulation suggests detectable changes in 13-year  
386 mean precipitation intensity in winter may emerge across the southern UK in the 2040s (Table  
387 2), which is in good agreement with the results of Fowler & Wilby (2010). Detection times are  
388 consistently earlier for hourly compared to daily precipitation, with differences of about 5-10  
389 years in the median detection year across the southern UK. Detection times are also generally  
390 earlier for precipitation averaged over larger spatial scales. A similar variation in detection time  
391 is seen for changes in heavy precipitation intensity ( $p_{95}$ ) in winter (Table 2). Changes in the top  
392 1% of all values ( $p_{99ALL}$ ) emerge later than changes in wet-value statistics (both mean  
393 precipitation intensity and  $p_{95}$ ), with  $p_{99ALL}$  reflecting changes in both the intensity and  
394 frequency of events. The 10<sup>th</sup> and 90<sup>th</sup> percentiles of the spatially varying estimates of detection  
395 year (in brackets in Table 2) typically span about 40-50 years, with changes in hourly  
396 precipitation emerging in the 2030s for some local regions. Maps showing the spatial  
397 variability in detection time (Figure 2) indicate that changes in heavy precipitation may be  
398 detected earlier towards the north and west in winter, perhaps suggestive of more westerly UK  
399 winters with climate change (Malby et al., 2007).

400

401 Changes in precipitation emerge later in summer compared to winter (Table 3). For daily  
402 precipitation intensity in summer, detectable changes have not even emerged by the end of the  
403 century. However, hourly and 10-minute precipitation changes emerge earlier by many  
404 decades. For heavy 10-minute precipitation intensity, results suggest detectable changes may  
405 typically emerge across the southern UK in the 2080s. Changes in the top 1% of all values  
406 ( $p_{99ALL}$ ) emerge considerably later than changes in wet-value statistics (both mean precipitation  
407 intensity and  $p_{95}$ ), due to large decreases in the frequency of rainfall in summer (Chan et al.,  
408 2014a) as least partially offsetting increases in rainfall intensity for all-value statistics. There  
409 is considerable spatial variability in the detection time in summer, with the 10<sup>th</sup> and 90<sup>th</sup>  
410 percentiles of the spatial estimates (in brackets in Table 3) spanning a century or more. Maps  
411 of detection time (Figure 2) indicate there is a less clear spatial pattern in detection time in  
412 summer compared to winter. Thus in summer there is considerable uncertainty in detection  
413 time; there may be some local regions where changes in short-duration heavy summertime  
414 precipitation emerge as early as the 2050s but others where there is no detectable change well  
415 beyond the end of this century.

416

417 We note that here a constant threshold of 0.1mm has been applied to define a wet value across  
418 all accumulation periods and spatial scales. It is easier to reach a 0.1mm accumulation over a  
419 day than over a 10-minute period. In particular, since rain typically lasts longer than 10-minutes  
420 (and, in winter, longer than an hour), the daily accumulation on days with 10-minute periods  
421 exceeding 0.1mm will likely be considerably higher than 0.1mm; whilst days just exceeding  
422 the 0.1mm threshold may likely contain no individual hours or 10-minute periods selected as  
423 wet. (Note this is only the case for the model results; for the observations where there is a  
424 minimum tip ranging from 0.1mm to 0.5mm depending on gauge, detailed in the  
425 supplementary information, if a day reports 0.1mm then there must be an hour with 0.1mm.)

426 This then raises the question whether the finding that 10-minute precipitation changes emerge  
427 earlier is simply due to the fact we are preferentially selecting the higher intensity events at  
428 shorter accumulation periods (although there will still be considerably more 10-minute wet  
429 periods than wet days in the 13 year simulation). Looking at detection times for changes in all-  
430 value statistics ( $p_{99ALL}$ ), however, shows this is not the case, with short-duration extremes  
431 consistently emerging earlier than daily extremes even when no wet-value threshold is applied.  
432 Also comparing detection times for precipitation intensity with those for heavy precipitation  
433 intensity ( $p_{95}$ ) shows that detection times are not always earlier for higher intensity events  
434 (Tables 2 and 3). Thus we argue it is the impact of increasing atmospheric moisture with  
435 warming, which tends to result in rainfall falling as fewer but more intense events, that gives  
436 greater increases in intensity at shorter-accumulation periods and hence favours the earlier  
437 detection of changes in 10-minute and hourly precipitation. For the analysis of observations in  
438 the following section we focus on changes in heavy precipitation intensity ( $p_{95}$ ), since these  
439 emerge earlier than all-day (and all-hour) extremes in the model. This is consistent with large  
440 decreases in rainfall occurrence (particularly in summer due to changing circulation patterns,  
441 Chan et al., 2014a) offsetting increases in rainfall intensity due to increasing atmospheric  
442 moisture. We note however that the detection time for all-day and all-hour extremes is  
443 important as this directly relates to when changes in flooding frequency will be detected (see  
444 Discussion).

445

446 Given these results are from single 13-year model realisations of the present and future climate,  
447 assume a linear trend through time, and do not account for multi-decadal natural variability  
448 (see Methods), we have low confidence in the actual detection years quoted. In particular,  
449 where detection times are beyond the end of the century, this reflects an extrapolation of the  
450 linear trend beyond the future simulation period and hence we have very low confidence in

451 these values especially given the projected profile of human-induced warming is far from linear  
452 over long periods. However, the finding that changes consistently emerge earlier for 10-minute  
453 compared to hourly compared to daily precipitation is expected to be more reliable. As noted  
454 above, it is consistent with the expected intensification of precipitation with climate change  
455 (Trenberth et al., 2003), such that changes in precipitation intensities are expected to be larger  
456 for shorter accumulation periods. This has been shown to be the case in summer in results from  
457 CPMs over both the UK and the Alps (Kendon et al., 2017). Results here suggest this greater  
458 signal of change dominates over any increases in noise associated with relatively greater natural  
459 variability at short timescales, at least where there is perfect sampling across space and time  
460 (but note, as discussed later, sampling issues in observational datasets may impact on this). We  
461 note variance estimates for the model control simulation agree well with observed variance for  
462 the 2002-2014 period, for both hourly and daily precipitation (Supplementary Tables S1 and  
463 S2), which gives credibility to the noise estimation that goes into the calculation of model  
464 detection time.

465

466 *b. Results from observed change analysis*

467 To examine results derived using the percentage change method we calculate the median of the  
468 percentage changes across all contributing gauges, to give a single central estimate across the  
469 UK, as well as the 10<sup>th</sup> and 90<sup>th</sup> percentiles of the spatially varying estimates to give an  
470 indication of uncertainty. Analysis of the results for  $p_{95}$  indicates significant spread in the  
471 magnitude of change across the gauges along with variation in the magnitude according to the  
472 periods used (Figure 3). For winter, most gauges indicate a decrease for the 2002-2014 period  
473 relative to preceding periods from those centred around 1980 onwards. In contrast, for summer,  
474 positive changes clearly emerge over the same periods, particularly for 24h accumulations. We  
475 note though that changes relative to earlier periods, particularly for summer, are characterised

476 by low gauge availability and so results are less robust. Similar patterns of changes are  
477 observed in the mean intensity (Figure S2) but with slightly smaller magnitude of change for  
478 summer over recent decades.

479

480 We then applied the normalised change method for three 13-year periods to more directly  
481 compare the observed changes with those from the model. The variability of each metric  
482 (obtained by resampling years in the 13-year start and end periods, see Section 2b) was used to  
483 calculate the statistic  $D_x$  where here the metric  $\mu_x$  refers to the latest 13-year period in the  
484 observations (i.e. the midpoint  $x$  is 2008) and  $\mu_c$  is the statistic for successive 13-year periods.  
485 The periods 1977-1989, 1983-1995 and 1989-2001 were selected to avoid the earlier part of  
486 the record with minimal numbers of gauges. Figure 4 shows the distribution of values of  $D_x$   
487 for the heavy precipitation intensity metric ( $p_{95}$ ). By comparison, the median  $D_x$  for the model  
488 for 100-year changes (mid year 2103 versus 2003) in  $p_{95}$  are 4.10 (2.08) for hourly precipitation  
489 at the 1.5km scale in DJF (JJA). Under the assumption that changes in  $p_{95}$  are linear through  
490 time, this would give a  $D_x$  value for the model for 25-year changes (mid-year 2028 versus 2003)  
491 of 1.03 (0.52) for hourly precipitation at the 1.5km scale in DJF (JJA). As shown in Figure 4,  
492 these model  $D_x$  values are within the 10<sup>th</sup> to 90<sup>th</sup> percentile ranges shown for the observations  
493 for a 25-year change (mid year 1983 versus 2008). Observed changes in Figure 4 are consistent  
494 with those for the percentage change in Figure 3. Winter changes in  $p_{95}$  are relatively modest  
495 and are similar for both 1h and 24h accumulations with a tendency for the period 2002-2014  
496 to show a decrease relative to periods from the early 1980s onwards. Again, for summer, the  
497 period 2002-2014 shows potentially larger increases emerging in daily accumulations  
498 compared with hourly. The magnitude of the estimated change is sensitive to the periods used  
499 but we reiterate that longer term changes are limited by gauge availability and so may not be  
500 representative. Comparable analyses for mean intensities (Figure S3) and for  $p_{99ALL}$  (Figure

501 S4), along with those for  $p_{95}$  using only those gauges in the model domain (Figure S5), do not  
502 appear to present qualitatively different results and so here we focus on the analysis of heavy  
503 precipitation intensity  $p_{95}$  using pooled gauges for the whole UK to maximise the detectability  
504 of change.

505

506 We next examined the spatial pattern of the normalised change in  $p_{95}$  to explore whether any  
507 regions might emerge as potential sentinels of a climate change signal. Fowler & Wilby (2010),  
508 for example, used RCM projections to suggest that SW England could be one such region for  
509 10 day winter precipitation totals with a 10-year return period. Here, the pattern of normalised  
510 change for hourly winter precipitation (relative to 1989-2001) is weak with some evidence of  
511 decreases tending to occur in the east (Figure S6a) whilst for summer the north and east of the  
512 UK show the strongest increases (Figure S6b). This latter pattern is replicated when compared  
513 with the period 1977-1989 but only 23 gauges are available and is also similar for daily  
514 precipitation though with a reduced regional contrast (not shown). The lack of long-term  
515 gauges means it is not possible to make robust inferences on the spatial pattern of change and  
516 so we do not consider this further in this analysis.

517

518 These results may be compared with those obtained using trends calculated using the maximum  
519 length of data available (long method) which shows that for gauges of >40 years length trends  
520 in mean winter rainfall intensity are largely positive (Figure S7a) though are not statistically  
521 significant at either the daily or hourly timescale. These positive trends are characteristic of  
522 those detected using the UK daily rain gauge network (see Section 1), however, in this analysis,  
523 over shorter, recent periods (calculated from 1980 onwards) a larger number of gauges exhibit  
524 contrasting non-significant negative trends. Comparing the mean of the relative Sen's slopes  
525 for 1h and 24h rainfall intensity (Figure S7) shows no clear pattern of a difference in trends

526 between the two timescales. This is confirmed by the absence of significant differences (95%  
527 level) signified by the Wilcoxon rank-sum test. A similar pattern is seen for trends in winter  
528  $p_{95}$ , with lower positive trends and more frequent negative trends over the most recent decades  
529 (Figure 5a, for relative trends, S8 and S9 for absolute trends). Using the 30y running trend  
530 analysis highlights even more clearly the (multi-) decadal scale variability and trend sensitivity  
531 to the period of analysis, showing a distinct shift from positive to negative trends from the  
532 period 1975-2004 onwards (Figure 5b).

533

534 As noted previously, summer is characterised by a particularly low number of gauges until  
535 ~1980 and so trends over earlier periods may not be representative of changes across the whole  
536 of the UK, however, more gauges generally exhibit (non-significant) positive trends throughout  
537 (Figure 6 for relative trends, S8-S11 for absolute trends). Another clear pattern that emerges  
538 is higher relative trends at both timescales from the 1980s onwards (Figure 6a), including the  
539 emergence of some trends that are statistically significant (Figures S8, S9). This is consistent  
540 with the analysis using the normalised change approach and with previous work by Simpson  
541 & Jones (2014) who noted that a series of wet summers starting in 2007 were beginning to  
542 offset a longer term downward trend in mean and extreme UK daily summer rainfall. During  
543 this later period, relative trends are also smaller for 1h than 24h accumulations, which is  
544 contrary to the CPM simulation and the observed scaling of hourly and daily rainfall with  
545 temperature (Chan et al., 2016a). Again, the 30y running trend analysis highlights trend  
546 variability, showing an increase in the mean intensity (Figure S12) and in  $p_{95}$  (Figure 6b for  
547 relative trends, S8 and S9 for absolute trends) trends for the 1985-2014 periods.

548

549 We reiterate the need for caution however in the interpretation of the temporal variability in  
550 trends observed in these figures. Figures 3, 5 and 6 indicate the relatively small number of



551 gauges for the early period. In particular, in summer all gauges contributing records for periods  
552 from 1970 and earlier are in Scotland or Northern Ireland (Figure 1) and so may only be  
553 indicative of regional change. Only from 1980 onwards are there significant number of gauges  
554 covering England and Wales. This problem is less pronounced in winter for which the longer  
555 gauges are more evenly spatially distributed across the UK but with northern and eastern  
556 England less well represented. To explore this further we recalculated the long trends using  
557 just those gauges that provide data for all periods from 1955 onwards for consistency, thus  
558 trends for each period were based on identical gauges albeit for a very small sample (DJF:11,  
559 JJA:5). Nonetheless, there is a degree of consistency with the complete sample of gauges. In  
560 winter there is a clear decrease in the trend for 1h heavy precipitation intensity (Figure S13a)  
561 but with a less clear response of 24h totals which shows a lower sensitivity to the calculation  
562 period. Summer (JJA) is especially constrained by the limitations noted above but there is a  
563 clear tendency for increasing trends (especially for 24h) over recent decades (Figure S13b).

564

### 565 *c. Potential contributors to trend variability*

566 The sensitivity of observed trends to the period of calculation suggests potential influence of  
567 natural variability and so here we investigate two natural modes of variability – the North  
568 Atlantic Oscillation (NAO) and the Atlantic Multidecadal Oscillation (AMO).

569 Figure 7a shows the previously documented positive phases of the winter NAO in the 1980s  
570 and 1990s and subsequent decrease in the index thereafter. The positive phase of the winter  
571 NAO is associated with wetter weather in northern Europe and so trends calculated from this  
572 period are likely influenced by increased precipitation at the start of the record, potentially  
573 contributing to the lower or even decreasing trends shown in Figures 4, 5, S8 and S9.  
574 Overlaying the mean running trends of  $p_{95}$  shows consistency with the smoothed NAO time  
575 series with a marked decrease in the period after the peak of the positive NAO phase.

576

577 The notable increase in recent summer trends also corresponds with a negative phase of the  
578 summer NAO (SNAO) (Figure 7b). This is consistent with previous literature suggesting  
579 significant negative correlation of the SNAO with summer rainfall over parts of the UK  
580 (Section 2c). Figure 7c also shows a strong increase in the summer AMO since the mid-1990s,  
581 again coincident with the increase in the magnitude of running trends and percentage change  
582 for summer  $p_{95}$ . The AMO has been noted to be linked to changes in the summer NAO, as well  
583 as recent wet summers over northern Europe (Section 2c). Thus overall, the observed trends in  
584  $p_{95}$  in summer appear to be strongly influenced by the NAO, which in turn may be related to  
585 the AMO. We also compared the teleconnection indices to variations in the ratio of the daily  
586 to hourly change in  $p_{95}$  but noted that this was relatively stable and appeared unrelated to  
587 variability in the NAO and AMO. This suggests that these modes of variability may not readily  
588 explain any differences in change between the two accumulation periods but further work  
589 might usefully investigate how natural variability affects the relative behaviour of extremes of  
590 different durations.

591

#### 592 **4. Discussion**

593 The results here suggest it is changes in precipitation intensity (or heavy precipitation intensity)  
594 that offer the greatest promise for detecting human influence on precipitation. Such changes  
595 are linked to increasing atmospheric moisture with warming and are expected to be robust  
596 across models. Changes in precipitation extremes measured using all-values are found here to  
597 consistently emerge later, due to these reflecting changes in intensity and frequency. However,  
598 it is these changes in intensity and frequency combined which will be felt in terms of flooding.  
599 Model results here suggest that changes in summertime urban flash flooding, which respond to  
600 changes in short-duration rainfall, may not be detected this century. Changes in fluvial

601 flooding, which respond to changes in more persistent rainfall, may be detected earlier where  
602 these are dominated by changes in wintertime precipitation extremes (specifically for daily  
603 precipitation extremes, the CPM here suggests changes emerge in the 2060s for  $p_{99ALL}$  for  
604 precipitation aggregated to the 50km scale, whilst Fowler and Wilby (2010) suggests 2040s for  
605 the 10 year return level).

606

607 It is important to note that the detection time methodology has only been applied here to a  
608 single realisation of future climate change from one climate model, and thus no estimate of  
609 modelling uncertainty in the quoted detection times is possible. Also, it has not been possible  
610 to account for the influence of multi-decadal natural variability from a single pair of 13-year  
611 control and future simulations. Additional ensemble CPM experiments will allow an  
612 assessment of the robustness of these results. In particular, the next set of UK climate  
613 projections, to be delivered in 2018 (UKCP18), will include the first ensemble of CPM  
614 simulations over the UK. This will allow a much better assessment of the influence of natural  
615 climate variability, including multi-decadal variability, and hence a more robust evaluation of  
616 detection time. Furthermore, coordinated multi-model ensemble experiments at convection  
617 permitting scale are being carried out across Europe as part of a CORDEX Flagship Pilot Study  
618 (FPS).

619

620 The results here correspond to using 13-years of data to calculate the metric for the control and  
621 future periods. Using more years of data, once these become available, would make detection  
622 of the change easier. In particular, where a continuous time series of data is available up to  
623 2050 and beyond (as will become available with time for observations, and for CPMs is  
624 planned under ongoing research at the UK Met Office beyond UKCP18), the metric could be

625 calculated for multiple (non-overlapping) periods and then detection of the change undertaken  
626 using all the data. This is likely to result in earlier detection times than those quoted here.

627

628 The first major study of change in UK sub-daily rainfall observations presented here provides  
629 some evidence of long-term increases in winter rainfall intensities as projected by the models.

630 In particular, these are evident in long trends for gauges with >40 years record, and are seen in  
631 percentage changes between the 2002-2014 and pre-1980 periods. However, these winter  
632 intensity increases are less consistent than extensive previous research on UK daily rainfall.

633 These results are however constrained here by the low number of long-term sub-daily gauges  
634 available for the analysis. The observations do also exhibit the emergence of recent increases  
635 in sub-daily heavy rainfall intensities in summer. However, the earlier emergence of detectable

636 changes in winter in the model is not seen in the observations, which may be explained by  
637 natural variability dominating observed trends at present. Also, in contrast with the CPM  
638 simulation, no consistent, significant difference between changes in 1h and 24h rainfall is

639 detected in either season. Barbero et al. (2017) similarly note an absence of the greater  
640 detectability of increases in hourly extremes compared with daily for US annual and seasonal  
641 maxima, except during winter. We consider that this lack of a difference between daily and

642 hourly trends compared with the CPM simulations could be due to a combination of:

- 643 • Relatively short records, particularly in summer, make trend detection more difficult  
644 due to a low signal-to-noise ratio.
- 645 • A relatively sparse network of rain gauges means that we are not able to adequately  
646 sample convective storms and their peak rainfall intensities on hourly timescales due to  
647 the limited spatial extent of events (Agel et al., 2015; Wasko et al., 2016). By contrast,  
648 winter extremes, albeit smaller in magnitude (Blenkinsop et al., 2017), are largely

649 driven by mid-latitude storms with large-scale synoptic forcing and are thus more  
650 consistent in space and better captured by the sparse gauge network.

651 • Barbero et al. (2017) also hypothesize that the measurement-interval truncation  
652 problem may also contribute to the lack of a trend in summer hourly extremes.  
653 Maximum hourly intensities over a day are likely to be truncated due to the fixed hourly  
654 intervals of precipitation measurement/recording, given that a typical convective event  
655 rarely peaks exactly between two clock hours. This effect is more limited at the daily  
656 timescale, as the life cycle of convective events generally does not exceed a few hours,  
657 and, generally falls within a day.

658 • The signature of natural variability in terms of daily versus hourly trends may be quite  
659 different from the signature of the underlying climate change signal. In particular, it  
660 may only be for the latter (which is not yet emerging in the observations) where hourly  
661 trends are expected to exceed daily trends.

662 The (largely non-significant) increase in summer rainfall intensities over the last three decades  
663 is notable and it may seem attractive to attribute this to thermodynamic (CC related) changes.  
664 However, the evidence presented here, coupled with previous research (e.g. Sutton & Dong,  
665 2012) suggests that natural variability, in part related to large scale modes of variability,  
666 potentially the NAO and AMO, are important drivers of extreme rainfall in the UK. This is  
667 supported by Brown (2017) which showed that the NAO dominates observed trends in UK  
668 summer daily rainfall extremes, in this case using a different observational dataset (the 25km  
669 gridded dataset prepared for UKCP09 based on many more daily gauges). Otto et al. (2015)  
670 attributed an increased risk of July 5-day rainfall extremes (but not June or August extremes)  
671 for England and Wales to anthropogenic change and suggested that the AMO is not the most  
672 important driver of increased precipitation. This may have been due to deficiencies in the  
673 model used in their analysis or may indicate the need to investigate other possible drivers (e.g.

674 Champion et al., 2015). Similarly, the increasing number of gauges displaying negative  
675 changes in winter shown by the percentage change and running trend analyses may be a  
676 consequence of a weakening of the positive phase of the NAO over recent decades, including  
677 a number of years when the NAO was in its negative phase towards the end of the analysis  
678 period. Such modes of variability may induce long-term persistence and further contribute to  
679 difficulties in identifying non-stationarity (Milly et al., 2015). Both change and trend analyses  
680 over these timescales are clearly sensitive to the period of record and for precipitation, which  
681 may be highly variable on decadal and multi-decadal timescales, care must be taken to consider  
682 the potential drivers of this variability rather than a casual inference of a potential climate  
683 change signal. A full attribution study is beyond the scope of this research but this does  
684 highlight the need to consider the contribution of large-scale dynamical *and* thermodynamic  
685 drivers to observed changes and natural variability in precipitation extremes. Furthermore,  
686 whilst it has been proposed that adaptation planning and engineering design for infrastructure  
687 be guided by the CC relationship (Zhang et al., 2017) understanding of this scaling needs to be  
688 coupled with an understanding of large-scale drivers (e.g. Pfahl et al., 2017). This will not  
689 only lead to improved attribution of changes but also to the improved use of models for  
690 seasonal predictions and long term projections.

691

692 Notwithstanding these caveats, historical observations remain essential for a better  
693 understanding of change and will aid the development of better projections of the future  
694 (Montanari & Koutsoyiannis, 2014; Milly et al., 2008) and there is a particular need to develop  
695 a global database for sub-daily precipitation data (Zhang et al., 2017). However, quantified  
696 estimates of observed changes and trends in precipitation metrics are on their own unlikely to  
697 provide sufficient understanding of, and evidence for, human-induced change for some time,  
698 at least at local/regional scales across most parts of the globe for some of the reasons noted

699 above. Robustly characterising and attributing observed changes in sub-daily extremes remains  
700 a considerable challenge. This is likely to be best addressed through the integrated use of high  
701 quality historical observations, not only of relevant surface weather variables but also of  
702 atmospheric variables, and the application of process-based models (Lenderink & Fowler,  
703 2017), taking advantage of ongoing developments in convection-permitting climate modelling  
704 (Prein et al., 2015), and analysis at continental scales. These challenges are currently being  
705 addressed by the INTENSE (INTElligent use of climate models for adaptatioN to non-  
706 Stationary hydrological Extremes) project. This project aims to establish increased synergy  
707 between data, models and theory to enable the development of new downscaling approaches,  
708 using information from climate models and process understanding from observations in a more  
709 intelligent way. In doing so we will be better able to understand how rainfall extremes will  
710 respond to a warmer world and the implications for adaptation strategies.

711

## 712 **5. Conclusion**

713 Results using output from a 1.5km convection-permitting climate model over the southern UK  
714 indicate that changes to 10-minute and 1h precipitation emerge before changes to daily  
715 precipitation. In particular, the model results suggest detection times in the 2040s for hourly  
716 rainfall intensity in winter, which are 5-10 years earlier than for daily extremes. In summer,  
717 detection times are typically in the 2080s for heavy 10-minute precipitation intensity, which is  
718 decades earlier than for daily extremes. However, there is considerable spatial variability in the  
719 detection time, particularly in summer. These results suggest that it is changes in rainfall rates,  
720 rather than changes to daily rainfall totals, which provide the greatest potential for detection of  
721 change. These could manifest in increases in pluvial flooding, which predominantly affect  
722 urban areas and small rapid-response catchments as flash floods. We note that it is in summer  
723 when the highest hourly precipitation extremes occur in the UK (Blenkinsop et al., 2017; Chan

724 et al., 2014a). So even though we may be able to detect changes in precipitation extremes in  
725 winter first, the detection of changes in summer is of considerable practical value particularly  
726 for the management of urban flash flooding. Hence the considerably earlier emergence of short-  
727 duration extremes compared to daily extremes in summer is important.

728

729 Results from a new quality-controlled dataset of hourly rainfall over the UK do not show a  
730 similar difference between daily and hourly changes. This appears to be explained by natural  
731 variability dominating trends in current observational records, although as warming  
732 strengthens the climate change signal may become more apparent. In general, the relative  
733 changes at hourly versus daily timescales may be a useful signature of underlying climate  
734 change that could be employed in detection and attribution studies. Although results presented  
735 here are for the UK, this signature is expected to apply more widely. In particular, where  
736 increasing atmospheric moisture with warming is the dominant driver of precipitation change,  
737 we may expect precipitation rates to intensify and the earlier emergence of detectable changes  
738 in short-duration precipitation intensities. There are also local feedbacks within storms, linked  
739 to latent heat release, which have been proposed to explain greater increases in rainfall  
740 extremes on hourly timescales (Lenderink & van Meijgaard, 2010; Lenderink et al., 2017) and  
741 are expected to apply more generally in convective regimes and seasons. This is consistent with  
742 the model results here showing that it is in summer, in particular, when hourly and sub-hourly  
743 extremes emerge much sooner than daily ones, as this is the season when convective storms  
744 are more prevalent.

745

746 Providing robust quantitative estimates of when we may be able to detect the influence of  
747 climate change on rainfall extremes is important for informing adaptation planning. The results  
748 presented here are from a single realisation of future climate change from one climate model,



749 and so we have low confidence in the actual detection years quoted. Providing robust estimates  
750 of detection time will require additional CPM ensemble experiments that are currently planned  
751 over the UK as part of the UKCP18 project and more widely as part of coordinated multi-model  
752 projects (e.g. CORDEX-FPS).

753

754 Current guidance on climate change allowances for rainfall for the purposes of UK flood risk  
755 management is provided by Defra (Defra, 2006) and the Environment Agency (Environment  
756 Agency, 2011), and specifies peak rainfall intensity increases of 5% (1990-2025), 10% (2025-  
757 2055), 20% (2055-2085) and 30% (2085-2115) relative to a 1961-90 baseline. However this  
758 guidance is not designed to be applied to sub-daily rainfall (the need for revised guidance is  
759 noted in Dale et. al., 2017). Results here suggest separate climate change allowances need to  
760 be developed for hourly and sub-hourly rainfall, the latter being particularly important for  
761 urban flash flooding. Such allowances will need to be specified for changes emerging over the  
762 next few decades. Thus future work will focus on exploiting the first ensemble of climate  
763 simulations at convection-permitting scale from UKCP18 to provide robust estimates of  
764 change in sub-daily rainfall extremes to inform updated national guidance on climate change  
765 allowances.

766

## 767 **6. Acknowledgements**

768 E.J. Kendon gratefully acknowledges funding from the Joint Department of Energy and  
769 Climate Change (DECC) and Department for Environment Food and Rural Affairs (Defra) Met  
770 Office Hadley Centre Climate Programme (GA01101). This work also forms part of a joint UK  
771 Met Office and Natural Environment Research Council (UKMO-NERC) funded project on  
772 Convective Extremes (CONVEX, NE/1006680/1) and the European Research Council funded  
773 INTENSE project (ERC-2013-CoG-617329). H.J. Fowler is also funded by the Wolfson

774 Foundation and the Royal Society as a Royal Society Wolfson Research Merit Award  
775 (WM140025) holder. We would like to thank Dr Renaud Barbero for conducting the  
776 assessment of the statistical tests for break points and Dr Steven Chan for contributing to the  
777 running of the climate model simulations.

778 **References**

- 779 Agel, L., Barlow M, Qian JH, Colby F, Douglas E, Eichler T, 2015. Climatology of daily  
780 precipitation and extreme precipitation events in the northeast United States,  
781 *J. Hydrometeorol.*, **16(6)**, 2537–2557.
- 782 Allen MR, Ingram WJ, 2002, "Constraints on future changes in climate and the hydrologic  
783 cycle" *Nature* **419** 224-232.
- 784 Archer DR, Fowler HJ, 2015. Characterising flash flood response to intense rainfall and  
785 impacts using historical information and gauged data in Britain. *J. Flood Risk*  
786 *Manage.* doi:10.1111/jfr3.12187.
- 787 Arnbjerg-Nielsen K, Willems P, Olsson J, Beecham S, Pathirana A, Bülow Gregersen I,  
788 Madsen H, Nguyen V T V, 2013. Impacts of climate change on rainfall  
789 extremes and urban drainage systems: a review. *Water Science and Technology*  
790 **68** 16-28.
- 791 Barbero R, Fowler HJ, Lenderink G, Blenkinsop S. 2017. Is the intensification of precipitation  
792 extremes with global warming better detected at hourly than daily resolutions?,  
793 *Geophys. Res. Lett.*, 43, doi:10.1002/2016GL071917.
- 794 Berg P, Moseley C, Haerter JO, 2013. Strong increase in convective precipitation in response  
795 to higher temperatures. *Nature Geosci.* 6, 181-185.
- 796 Blenkinsop S, Chan SC, Kendon EJ, Roberts NM, Fowler HJ, 2015. Temperature influences  
797 on intense UK hourly precipitation and dependency on largescale circulation.  
798 *Environ. Res. Lett.*, 10, 054021.
- 799 Blenkinsop S, Lewis E, Chan SC, Fowler HJ, 2017. An hourly precipitation dataset and  
800 climatology of extremes for the UK. *International Journal of Climatology*, **37**,  
801 722–740.

802 Brown S, 2017. The drivers of variability in UK extreme rainfall. *International Journal of*  
803 *Climatology*, doi:10.1002/joc.5356.

804 Cabinet Office & DEFRA, 2016. National Flood Resilience Review, HM Government,  
805 pp145.

806 Champion AJ, Allan RP, Lavers DA, 2015. Atmospheric rivers do not explain UK summer  
807 extreme rainfall. *J. Geophys. Res. Atmos.*, **120**, 6731–6741.

808 Chan, S. C., E. J. Kendon, H. J. Fowler, S. Blenkinsop, C. A. T. Ferro, and D. B. Stephenson,  
809 2013. Does increasing the spatial resolution of a regional climate model  
810 improve the simulated daily precipitation? *Climate Dyn.*, 41, 1475–1495,  
811 doi:10.1007/s00382-012-1568-9.

812 Chan, S. C., E. J. Kendon, H. J. Fowler, S. Blenkinsop, and N. M. Roberts, 2014a: Projected  
813 increases in summer and winter UK sub-daily precipitation extremes from high  
814 resolution regional climate models. *Environ. Res. Lett.*, 9, 084 019,  
815 doi:10.1088/1748-9326/9/8/084019.

816 Chan S.C., Kendon E.J., Fowler H.J., Blenkinsop S., Roberts N., Ferro C.A.T., 2014b. The  
817 value of high-resolution Met Office regional climate models in the simulation  
818 of multi-hourly precipitation extremes. *Journal of Climate*, **27**, 6155-6174.

819 Chan SC, Kendon EJ, Roberts NM, Fowler HJ, Blenkinsop S. 2016a. Downturn in scaling of  
820 UK extreme rainfall with temperature for future hottest days. *Nature Geosci.*,  
821 9, 24-28.

822 Chan SC, Kendon EJ, Roberts NM, Fowler HJ, Blenkinsop S, 2016b. The characteristics of  
823 summer sub-hourly rainfall over the southern UK in a high-resolution  
824 convective permitting model. *Env. Res. Lett.*, **11**, 094024.

825 Dale, M., B. Luck, H.J. Fowler, S. Blenkinsop, E. Gill, J. Bennett, E.J. Kendon, S.C. Chan,  
826 2017. New climate change rainfall estimates for sustainable drainage, 170 (4)

827 (August 2017; themed issue on sustainable adaptation - part 1) Engineering  
828 Sustainability, doi:10.1680/jensu.15.00030

829 Darch GJC, McSweeney RT, Kilsby CG, Jones PG, Osborn TJ, Tomlinson JE, 2016.  
830 Analysing changes in short-duration extreme rainfall events. Proceedings of  
831 the Institution of Civil Engineers - Water Management, **169**, 201-211

832 Defra, 2006. Flood and Coastal Defence Appraisal Guidance FCDPAG3 Economic Appraisal  
833 – Supplementary note to operating authorities – climate change impacts, s.I.:  
834 Defra

835 Enfield, D.B., A.M. Mestas-Nunez, and P.J. Trimble, 2001: The Atlantic Multidecadal  
836 Oscillation and its relationship to rainfall and river flows in the continental  
837 U.S., *Geophys. Res. Lett.*, **28**, 2077-2080.

838 Environment Agency, 2011. Adapting to climate change: advice for flood and coastal erosion  
839 risk management authorities, Environment Agency.

840 Faulkner, D.S., 1999. Rainfall frequency estimation. Volume 2 of the *Flood Estimation*  
841 *Handbook*. Centre for Ecology & Hydrology.

842 Fischer EM, Knutti R, 2016. Observed heavy precipitation increase confirms theory and early  
843 models. *Nature Clim. Change*, **6**, 986-991.

844 Folland, CK, Knight J, Linderholm HW, Fereday D, Ineson S, Hurrell JW, 2009. The Summer  
845 North Atlantic Oscillation: Past, Present, and Future. *J. Climate*, **22**, 1082–  
846 1103,

847 Fowler HJ, Kilsby CG. 2003a. A regional frequency analysis of United Kingdom extreme  
848 rainfall from 1961 to 2000. *International Journal of Climatology* **23**: 1313-  
849 1334.

850 Fowler HJ, Kilsby CG. 2003b. Implications of changes in seasonal and annual extreme rainfall.  
851 *Geophysical Research Letters* **30**: 1720.

852 Fowler HJ, Cooley D, Sain SR, Thurston M, 2010. Detecting change in UK extreme  
853 precipitation using results from the climateprediction.net BBC Climate Change  
854 Experiment. *Extremes*, **13(2)**, 241-267, doi:10.1007/s10687-010-0101-y.

855 Fowler HJ, Wilby RL, 2010. Detecting changes in seasonal precipitation extremes using  
856 regional climate model projections: Implications for managing fluvial flood  
857 risk. *Water Resources Research*, **46**, W03525.

858 Hamlington BD, Leben RR, Strassburg MW, Nerem RS, Kim K.-Y., 2013. Contribution of the  
859 Pacific Decadal Oscillation to global mean sea level trends, *Geophys. Res.*  
860 *Lett.*, **40**, 5171–5175, doi:10.1002/grl.50950.

861 Hegerl GC, Black E, Allan RP, Ingram WJ, Polson D, Trenberth KE, Chadwick RS, Arkin PA,  
862 Sarojini BB, Becker A, Dai A, Durack PJ, Easterling D, Fowler HJ, Kendon  
863 EJ, Huffman GJ, Liu C, Marsh R, New M, Osborn TJ, Skliris N, Stott PA,  
864 Vidale PL, Wijffels SE, Wilcox LJ, Willett KM, Zhang X. 2015. Challenges  
865 in Quantifying Changes in the Global Water Cycle. *Bull. Amer. Meteor. Soc.*,  
866 **96**: 1097–1115, doi: 10.1175/BAMS-D-13-00212.1.

867 Hoy, A., Schucknecht, A., Sepp, M., Matschullat J, 2014. Large-scale synoptic types and  
868 their impact on European precipitation. *Theor Appl Climatol*, **116**, 19-35.

869 Hurrell, JW, 1995. Decadal Trends in the North Atlantic Oscillation: Regional Temperatures  
870 and Precipitation. *Science*, **269**, 676-679.

871 Hurrell, JW, 1996. Influence of variations in extratropical wintertime teleconnections on  
872 northern hemisphere temperature. *Geophysical Research Letters*, **23**, 665-668.

873 Hurrell JW, Kushnir Y, Ottersen G, Visbeck M. 2003. An overview of the North Atlantic  
874 Oscillation. The North Atlantic Oscillation: climatic significance and  
875 environmental impact. *Geophysical Monograph*, **134**, 1–35.

876 Jassby AD, Cloern JE, 2016. wq: Some tools for exploring water quality monitoring data. R  
877 package version 0.4.7. <http://cran.r-project.org/package=wq>.

878 Jenkins GJ, Perry MC, Prior MJ. 2008. *The climate of the United Kingdom and recent trends*.  
879 Met Office Hadley Centre, Exeter, UK.

880 Jones MR, Fowler HJ, Kilsby CG, Blenkinsop S. 2013. An assessment of changes in seasonal  
881 and annual extreme rainfall in the UK between 1961 and 2009. *International*  
882 *Journal of Climatology* **33**: 1178–1194.

883 Jones, P.D., Jónsson, T. and Wheeler, D., 1997: Extension to the North Atlantic Oscillation  
884 using early instrumental pressure observations from Gibraltar and South-West  
885 Iceland. *Int. J. Climatol.*, **17**, 1433-1450.

886 Kendon E.J., Roberts N.M., Senior C.A., Roberts M.J., 2012. Realism of rainfall in a very high  
887 resolution regional climate model. *Journal of Climate*, **25**, 5791-5806.

888 Kendon EJ, Roberts NM, Fowler HJ, Roberts MJ, Chan SC, Senior CA, 2014. Heavier summer  
889 downpours with climate change revealed by weather forecast resolution model.  
890 *Nature Clim. Change*, **4**, 570–576.

891 Kendon EJ, Ban N, Roberts NM, Fowler HJ, Roberts MJ, Chan SC, Evans JP, Fosser G,  
892 Wilkinson JM, 2017. Do convection-permitting regional climate models  
893 improve projections of future precipitation change? *BAMS.*, **98** (1), 79-, doi:  
894 10.1175/BAMS-D-15-0004.1.

895 Lean, H.W., P.A. Clark, M. Dixon, N.M. Roberts, A. Fitch, R. Forbes, and C. Halliwell,  
896 2008. Characteristics of high-resolution versions of the Met Office Unified  
897 Model for forecasting convection over the United Kingdom, *Mon. Weather*  
898 *Rev.*, 136, 3408--3424, doi:10.1175/2008MWR2332.1

899 Lenderink G, Fowler HJ, 2017. Hydroclimate: Understanding Precipitation Extremes. *Nature*  
900 *Climate Change*, doi:10.1038/nclimate3305.

901 Lenderink G, van Meijgaard E. 2008. Increase in hourly precipitation extremes beyond  
902 expectations from temperature changes, *Nat. Geosci.*, **1**, 511–514.

903 Lenderink G, van Meijgaard E. 2010. Linking increases in hourly precipitation extremes to  
904 atmospheric temperature and moisture changes, *Environ. Res. Lett.*, **5**(2),  
905 025,208.

906 Lenderink, G., Barbero, R., Loriaux, J.M., Fowler, H.J. 2017. Super Clausius-Clapeyron  
907 scaling of extreme hourly precipitation and its relation to large-scale  
908 atmospheric conditions. *Journal of Climate*, DOI: 10.1175/JCLI-D-16-0808.1

909 Lewis E, Quinn N, Blenkinsop S, Freer J, Fowler HJ, Coxon, Bates, Woods, 2017. A gridded  
910 hourly precipitation dataset for the UK. Submitted, *Journal of Hydrology*.

911 Linderholm, H. W., Folland, C. K. and Walther, A. (2009), A multicentury perspective on the  
912 summer North Atlantic Oscillation (SNAO) and drought in the eastern Atlantic  
913 Region. *J. Quaternary Sci.*, **24**, 415–425.

914 Lohmann K, Drange H, Bentsen M, 2009. Response of the North Atlantic subpolar gyre to  
915 persistent North Atlantic oscillation like forcing. *Climate Dynamics*, **32**, 273-  
916 285.

917 Loriaux JM, Lenderink G, De Roode SR, Siebesma AP, 2013. Understanding Convective  
918 Extreme Precipitation Scaling Using Observations and an Entraining Plume  
919 Model. *Journal of the Atmospheric Sciences*, **70**, 3641-3655.

920 Malby AR, Whyatt JD, Timmis RJ, Wilby RL, Orr HG, 2007. Long-term variations in  
921 orographic rainfall: analysis and implications for upland catchments.  
922 *Hydrological Sciences Journal*, 52(2):276-91.

923 Maraun D, Osborn TJ, Gillett NP. 2008. United Kingdom daily precipitation intensity:  
924 improved early data, error estimates and an update from 2000 to 2006.  
925 *International Journal of Climatology* **28**: 833-842.



926 Milly PCD, Betancourt J, Falkenmark M, Hirsch RM, Kundzewicz ZW, Lettenmaier DP,  
927 Stouffer RJ, 2008. Stationarity Is Dead: Whither Water Management? *Science*,  
928 **319**, 573-574. doi: 10.1126/science.1151915.

929 Milly PCD, Betancourt J, Falkenmark M, Hirsch RM, Kundzewicz ZW, Lettenmaier DP,  
930 Stouffer RJ, Dettinger MD, Krysanova V, 2015. On Critiques of “Stationarity  
931 is Dead: Whither Water Management?” *Water Resources Research*, **51**, 7785-  
932 7789. doi:10.1002/2015WR017408.

933 Min S-K, Zhang X, Zwiers F W, Hegerl G C, 2011. Human contribution to more-intense  
934 precipitation extremes. *Nature* **470** 378-381.

935 Mishra V, Wallace JM, Lettenmaier DP, 2012. Relationship between hourly extreme  
936 precipitation and local air temperature in the United States, *Geophys. Res. Lett.*,  
937 **39**, L16403.

938 Montanari A, Koutsoyiannis D, 2014. Modeling and mitigating natural hazards: Stationarity is  
939 immortal!" *Water Resources Research*, **50**, 9748-9756.  
940 doi:10.1002/2014WR016092.

941 Murphy JM, Sexton DMH, Jenkins GJ, Boorman PM, Booth BBB, Brown CC, Clark RT,  
942 Collins, M., Harris GR, Kendon EJ, Betts RA, Brown SJ, Howard TP,  
943 Humphrey KA, McCarthy MP, McDonald RE, Stephens A, Wallace C, Warren  
944 R, Wilby R, Wood RA, 2009. *UK Climate Projections Science Report: Climate  
945 change projections*. Met Office Hadley Centre, Exeter.

946 Osborn TJ, Hulme M. 2002. Evidence for trends in heavy rainfall events over the UK.  
947 *Philosophical Transactions of the Royal Society of London. Series A:*  
948 *Mathematical, Physical and Engineering Sciences* **360**: 1313-1325.

949 Osborn TJ, Hulme M, Jones PD, Basnett TA. 2000. Observed trends in the daily intensity of  
950 United Kingdom precipitation. *International Journal of Climatology* **20**: 347-  
951 364.

952 Otto FEL, Rosier SM, Allen MR, Massey NR, Rye CJ, Quintana JI, 2015. Attribution analysis  
953 of high precipitation events in summer in England and Wales over the last  
954 decade. *Climatic Change*, **132** 77-91.

955 Pall P, Allen M R, Stone D A, 2007, "Testing the Clausius–Clapeyron constraint on changes  
956 in extreme precipitation under CO2 warming" *Climate Dynamics* **28** 351-363.

957 Pall P, Aina T, Stone D A, Stott P A, Nozawa T, Hilberts A G J, Lohmann D, Allen M R,  
958 2011, Anthropogenic greenhouse gas contribution to flood risk in England  
959 and Wales in autumn 2000. *Nature* **470** 382-385. doi:10.1038/nature09762.

960 Pfahl S, Ogorman PA, Fischer EM, 2017. Understanding the regional pattern of projected  
961 future changes in extreme precipitation. *Nature Clim. Change*,  
962 doi:10.1038/nclimate3287.

963 Prein AF, Langhans W, Fosser G, Ferrone A, Ban N, Goergen K, Keller M, Tölle M, Gutjahr  
964 O, Feser F, Brisson E, Kollet S, Schmidli J, van Lipzig NPM, Leung R, 2015. A  
965 review on regional convection-permitting climate modeling: Demonstrations,  
966 prospects, and challenges, *Rev. Geophys.*, **53**, 323–361.

967 Risbey JS, Lewandowsky S, Langlais C, Monselesan DP, O’Kane TJ, Oreskes N, 2014. Well-  
968 estimated global surface warming in climate projections selected for ENSO  
969 phase. *Nature Clim. Change*, **4**, 835-840. doi:10.1038/nclimate2310.

970 Robson J, Sutton R, Lohmann K, Smith D, Palmer MD, 2012: Causes of the Rapid Warming  
971 of the North Atlantic Ocean in the Mid-1990s. *J. Climate*, **25**, 4116–4134.

972 Santer BD, Bonfils C, Painter JF, Zelinka MD, Mears C, Solomon S, Schmidt GA, Fyfe JC,  
973 Cole JN S, Nazarenko L, Taylor KE, Wentz FJ, 2014. Volcanic contribution

974 to decadal changes in tropospheric temperature. *Nature Geosci.* **7** 185-189.  
975 doi:10.1038/ngeo2098.

976 Sarojini BB, Stott PA, Black E. 2016. Detection and attribution of human influence on regional  
977 precipitation. *Nature Climate Change* **6**: 669-675.

978 Schaller N, Kay A L, Lamb R, Massey N R, van Oldenborgh G J, Otto F E L, Sparrow S N,  
979 Vautard R, Yiou P, Ashpole I, Bowery A, Crooks S M, Haustein K,  
980 Huntingford C, Ingram W J, Jones R G, Legg T, Miller J, Skeggs J, Wallom D,  
981 Weisheimer A, Wilson S, Stott P A, Allen M R, 2016. Human influence on  
982 climate in the 2014 southern England winter floods and their impacts. *Nature*  
983 *Clim. Change*, **6**, 627-634.

984 Sen PK, 1968. Estimates of the regression coefficient based on Kendall's tau. *Journal of the*  
985 *American Statistical Association*, **63**, 1379–1389, doi:10.2307/2285891.

986 Simpson IR, Jones PD, 2014. Analysis of UK precipitation extremes derived from Met Office  
987 gridded data. *International Journal of Climatology* **34**: 2438–2449.

988 Stein THM, Hogan RJ, Clark PA, Halliwell CE, Hanley KE, Lean HW, Nicol JC and Plant RS,  
989 2015. The DYMECS Project: A Statistical Approach for the Evaluation of  
990 Convective Storms in High-Resolution NWP Models, *Bull. Am. Meteorol. Soc.*  
991 **96**, 939–951

992 Sutton RT, Dong B, 2012. Atlantic Ocean influence on a shift in European climate in the 1990s.  
993 *Nature Geosci.*, **5**, 788-792.

994 Theil H, 1950. A rank-invariant method of linear and polynomial regression analysis. *I. Proc.*  
995 *Kon. Ned. Akad. v. Wetensch. Ser A53*, 386-392 (Part I), 521-525 (Part II),  
996 1397-1412 (Part III).

997 Trenberth KE, Dai A, Rasmussen RM, Parsons DB, 2003. The changing character of  
998 precipitation. *Bull. Amer. Meteor. Soc.*, **84**, 1205–1217.

999 Trigo RM, Osborn TJ, Corte-Real J, 2002. The North Atlantic Oscillation influence on Europe:  
1000 climate impacts and associated physical mechanisms. *Climate Research*, **20**, 9-  
1001 17.

1002 Trottini M, Isabel M, Aguiar V, Palazón SB, 2015: On the Use of Running Trends as Summary  
1003 Statistics for Univariate Time Series and Time Series Association. *J. Climate*,  
1004 **28**, 7489–7502, doi: 10.1175/JCLI-D-15-0009.1.

1005 Walker GT (1924) Correlations in seasonal variations of weather. IX Mem Ind Meteorol  
1006 Dept, **24**:275–332.

1007 Walters, D.N., M.J. Best, A.C. Bushell, D. Copsey, J.M. Edwards, P.D. Falloon, C.M. Harris,  
1008 A.P. Lock, J.C. Manners, C.J. Morcrette, M.J. Roberts, R.A. Stratton, S.  
1009 Webster, J.M. Wilkinson, M.R. Willett, I.A. Boutle, P.D. Earnshaw, P.G.  
1010 Hill, C.MacLachlan, G.M. Martin, W. Moufouma-Okia, M.D. Palmer, J.C.  
1011 Petch, G.G. Rooney, A.A. Scaife, and K.D. Williams, 2011. The Met Office  
1012 Unified Model global atmosphere 3.0/3.1 and JULES global land 3.0/3.1  
1013 configurations. *Geosci. Model Devel.*, 4, 919--941, doi:10.5194/gmd-4-919-  
1014 2011.

1015 Wasko, C., Sharma A, Westra S, 2016. Reduced spatial extent of extreme storms at higher  
1016 temperatures, *Geophys. Res. Lett.*, **43**, 4026–4032.

1017 Westra S, Fowler HJ, Evans JP, Alexander LV, Berg P, Johnson F, Kendon EJ, Lenderink G,  
1018 Roberts NM, 2014. Future changes to the intensity and frequency of short-  
1019 duration extreme rainfall, *Rev. Geophys.*, 52,522–555,  
1020 doi:10.1002/2014RG000464.

1021 Westra S, Sisson SA, 2011. Detection of non-stationarity in precipitation extremes using a  
1022 max-stable process model. *Journal of Hydrology*, **406**, 119-128.  
1023 doi:10.1016/j.jhydrol.2011.06.014.

1024 Wilby, R. L., O'Hare, G. and Barnsley, N., 1997. The North Atlantic Oscillation and British  
1025 Isles climate variability, 1865–1996. *Weather*, **52**, 266–276.

1026 Wilby RL, Conway D, Jones PD, 2002. Prospects for downscaling seasonal precipitation  
1027 variability using conditioned weather generator parameters. *Hydrol. Process.*,  
1028 **16**, 1215–1234.

1029 Zhang X, Zwiers FW, Li G, Wan H, Cannon AJ, 2017. Complexity in estimating past and future  
1030 extreme short-duration rainfall. *Nature Geoscience*, **10**, 255–259.  
1031 doi:10.1038/ngeo2911.

1032

1033

1034

<b>Period</b>	<b>DJF</b>	<b>JJA</b>
<b>Percentage/normalised change</b>	108	115
<b>Long trends</b>	63	72
<b>Running trends</b>	73	78
<b>Combined unique</b>	123	130

1035

1036 Table 1: Number of gauges available for each season and for each method used for the  
1037 analysis of change. The total number of unique gauges is also shown.

1038

1039

	<b>1.5km</b>	<b>5km</b>	<b>12km</b>	<b>50km</b>
<b>Precipitation intensity</b>				
daily	2050 (2033, 2086)	2051 (2033, 2090)	2051 (2034, 2092)	2050 (2033, 2100)
hrly	2048 (2034, 2071)	2046 (2034, 2073)	2045 (2034, 2075)	2041 (2032, 2060)
<b>Heavy precipitation intensity <math>p_{95}</math></b>				
daily	2056 (2042, 2084)	2056 (2042, 2085)	2055 (2041, 2084)	2054 (2040, 2077)
hrly	2051 (2032, 2073)	2050 (2032, 2072)	2048 (2032, 2069)	2042 (2032, 2061)
<b>Heavy precipitation <math>p_{99ALL}</math></b>				
daily	2071 (2048, 2117)	2070 (2048,2115)	2069 (2048,2112)	2061 (2044,2098)
hrly	2055 (2033,2084)	2055 (2033,2082)	2053 (2034,2078)	2050 (2034,2071)

1040

1041 Table 2: Median detection year across southern UK land points for changes in (top)  
1042 precipitation intensity, (middle) heavy precipitation intensity  $p_{95}$  and (bottom) heavy  
1043 precipitation  $p_{99ALL}$  in winter, for precipitation accumulated across a range of space (1.5km-  
1044 50km) and time (hrly-daily) scales. Also shown in brackets are the 10<sup>th</sup> and 90<sup>th</sup> percentiles of  
1045 the spatially varying estimates of detection year. Precipitation intensity is defined as the mean  
1046 of wet values ( $>0.1$ mm per accumulation period) over the 13-year period, heavy precipitation  
1047 intensity is defined as the mean of the upper 5% of wet values ( $p_{95}$ ), and heavy precipitation is  
1048 defined as the mean of the upper 1% of all values ( $p_{99ALL}$ ).

	<b>1.5km</b>	<b>5km</b>	<b>12km</b>	<b>50km</b>
<b>Precipitation intensity</b>				
daily	2252 (2117, 3211)	2261 (2119, 3247)	2261 (2124, 3426)	2325 (2129, 4195)
hrly	2123 (2078, 2299)	2121 (2076, 2315)	2116 (2072, 2289)	2121 (2079, 2314)
10min	2107 (2072, 2198)	2100 (2068, 2186)	2093 (2062, 2171)	2114 (2069, 2187)
<b>Heavy precipitation intensity <math>p_{95}</math></b>				
daily	2178 (2095, 2814)	2186 (2099, 2858)	2210 (2107, 3027)	2266 (2138, 2874)
hrly	2097 (2064, 2182)	2095 (2062, 2179)	2096 (2062, 2188)	2126 (2085, 2257)
10min	2088 (2059, 2157)	2083 (2054, 2146)	2091 (2056, 2179)	2184 (2084, 2543)
<b>Heavy precipitation <math>p_{99ALL}</math></b>				
daily	2308 (2126,3625)	2320 (2128,3617)	2314 (2131,3514)	2329 (2127,3006)
hrly	2175 (2092,2744)	2188 (2097,2821)	2205 (2105,2974)	2211 (2124,5058)
10min	2107 (2069,2224)	2119 (2075,2273)	2147 (2088,2454)	2211 (2121,3572)

1049

1050 Table 3: As Table 2, but for changes in (top) precipitation intensity, (middle) heavy  
1051 precipitation intensity  $p_{95}$  and (bottom) heavy precipitation  $p_{99ALL}$  in summer. In this season,  
1052 results are also available for 10-minute precipitation.

1053



1054 **Figure caption list**

1055 Figure 1: Sub-daily rain gauges included in the analyses for a) DJF (123 gauges), and b) JJA  
1056 (130 gauges). Years denote the first year in the earliest 13y analysis period meeting  
1057 the required level of completeness. Line denotes northern limit of the CPM simulation  
1058 domain.

1059 Figure 2: Spatial variation in detection year across the southern UK for changes in heavy  
1060 precipitation intensity  $p_{95}$  in (left) winter and (right) summer, for hourly precipitation  
1061 at 5km scale. Heavy precipitation intensity is defined as the mean of the upper 5% of  
1062 wet values ( $p_{95}$ ).

1063 Figure 3: Percentage change in heavy rainfall intensity ( $\Delta p_{95}$ ) for the period 2002-2014 relative  
1064 to successive rolling 13-year periods in the observations (top row 1h, middle row  
1065 24h). Change is plotted at the midpoint of the earlier 13-year period. The solid line  
1066 denotes the median of the change across all available gauges, the shading denotes the  
1067 range bounded by the 10<sup>th</sup> and 90<sup>th</sup> percentile ranges where at least 15 gauges are  
1068 available. The horizontal lines indicate the periods used to resample the observed  
1069 time series to evaluate normalised change. The bar plots (bottom row) denote the  
1070 number of gauges available for each period.

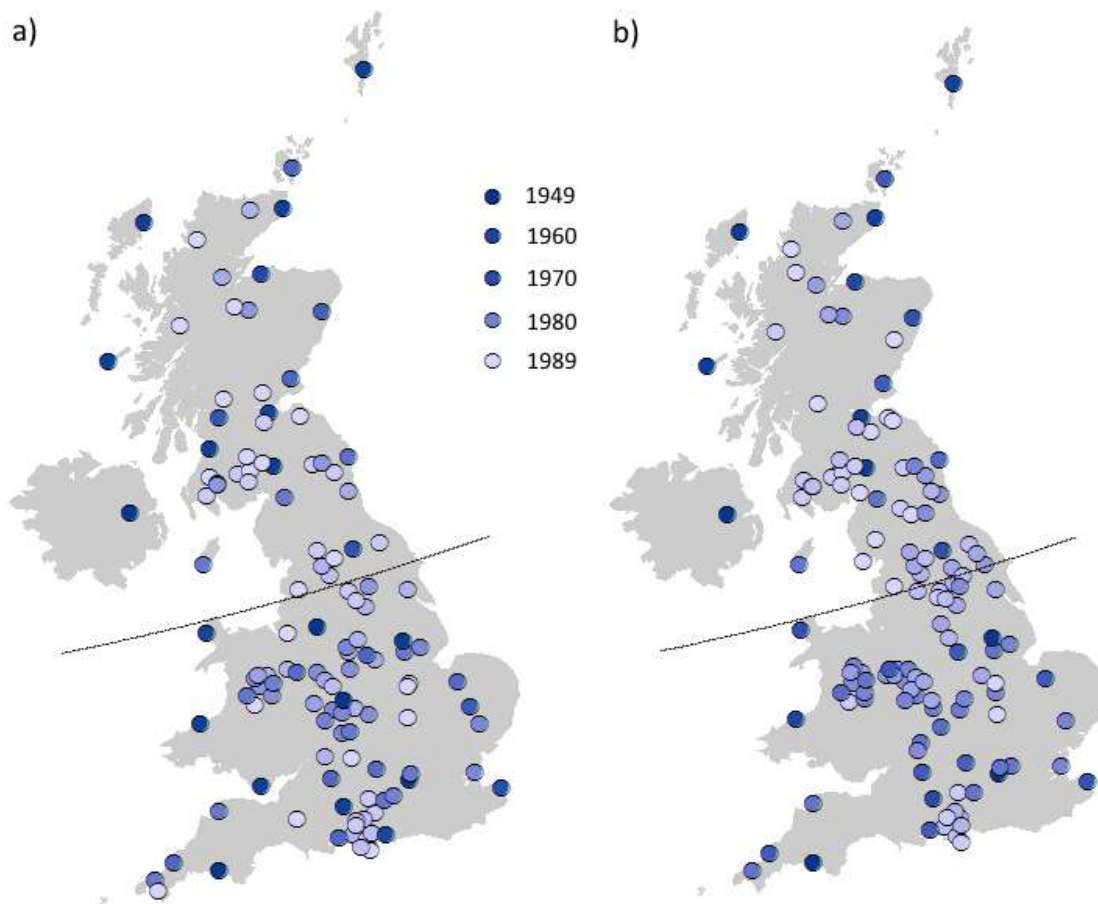
1071 Figure 4: Distribution of normalised change in heavy rainfall intensity ( $p_{95}, D_x$ ) for 1h and 24h  
1072 accumulations for the period 2002-2014 relative to three 13 year periods in the  
1073 observations. The black triangles denote the median of the corresponding 1.5km model  
1074 results for a 25-year change (scaled linearly from the 100-year change). The value  $n$  denotes  
1075 the number of gauges available for each period used to calculate change.

1076 Figure 5: Relative Sen's slope (unitless) for winter (DJF) hourly and daily heavy rainfall  
1077 intensity ( $p_{95}$ ) in the observations for a) successive periods ending in 2014 (long

1078 trends) and b) successive 30y periods (running trends). Points show mean slope of  
1079 all gauges whilst ranges show the 95% confidence interval estimated using the  
1080 Student's t distribution when the number of gauges  $n \geq 15$  (see Supporting  
1081 Information for method details). Lower plots shows the number of gauges used for  
1082 each period.

1083 Figure 6: As in Figure 5 but for summer (JJA) hourly and daily heavy rainfall intensity ( $p_{95}$ ) in  
1084 the observations.

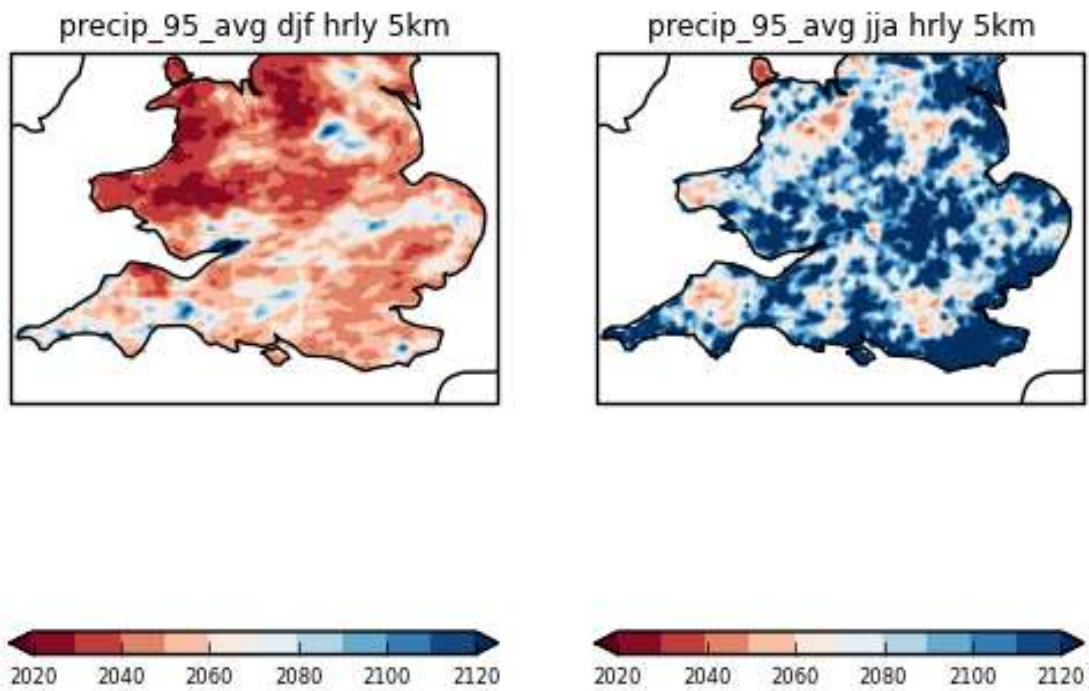
1085 Figure 7: Time series of teleconnection indices for a) DJF NAO, b) JJA NAO, c) JJA AMO.  
1086 The black line denotes the 15-year moving average. The orange and green lines  
1087 indicate the mean seasonal relative Sen's slope for 1h and 24h  $p_{95}$  using running  
1088 trends for each 30-year period plotted at the mid-year.



1090

1091 Figure 1: Sub-daily rain gauges included in the analyses for a) DJF (123 gauges), and b) JJA  
 1092 (130 gauges). Years denote the first year in the earliest 13y analysis period meeting  
 1093 the required level of completeness. Line denotes northern limit of the CPM simulation  
 1094 domain.

1095



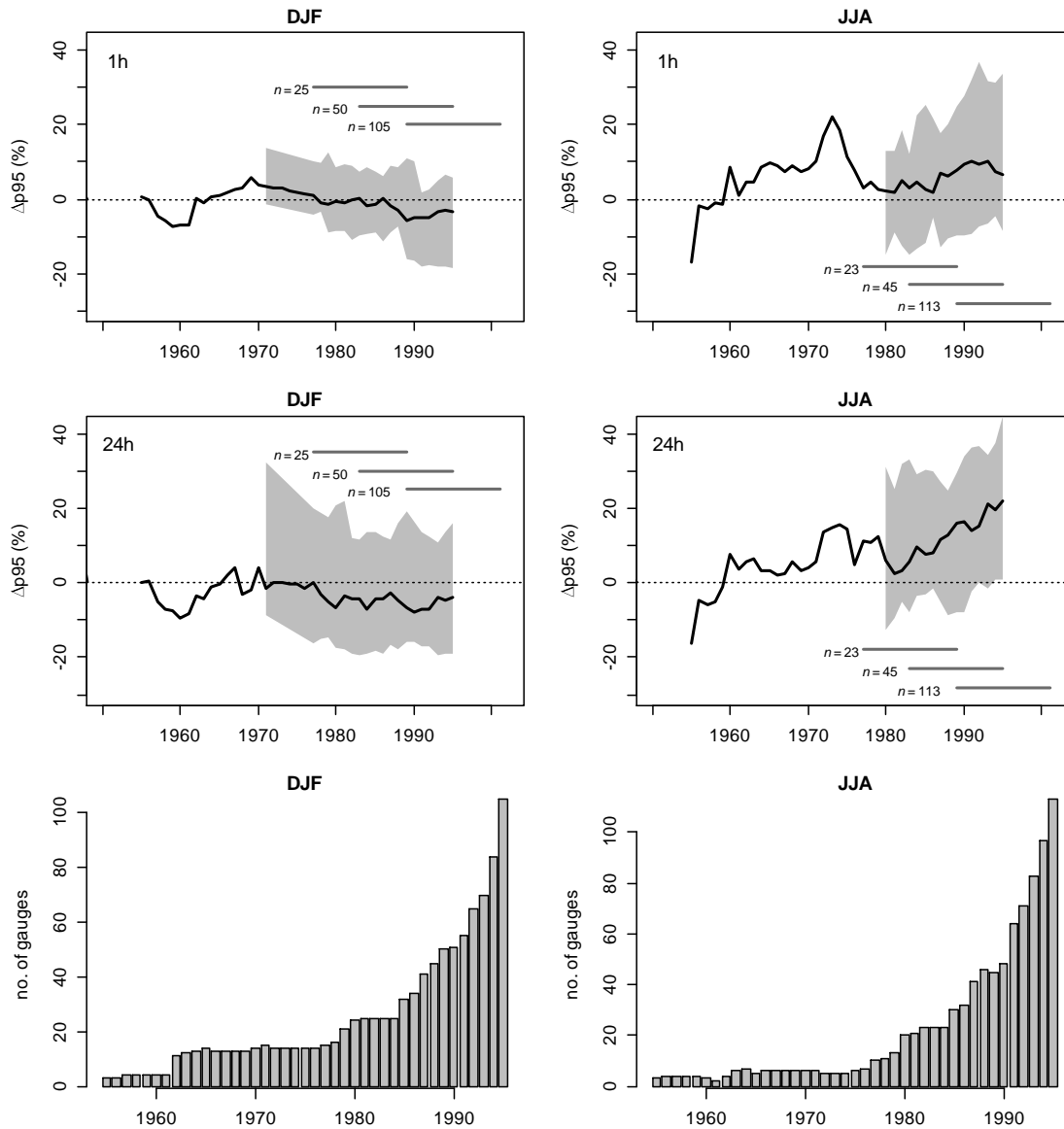
1096

1097

1098 Figure 2: Spatial variation in detection year across the southern UK for changes in heavy  
 1099 precipitation intensity  $p_{95}$  in (left) winter and (right) summer, for hourly precipitation  
 1100 at 5km scale. Heavy precipitation intensity is defined as the mean of the upper 5% of  
 1101 wet values ( $p_{95}$ ).

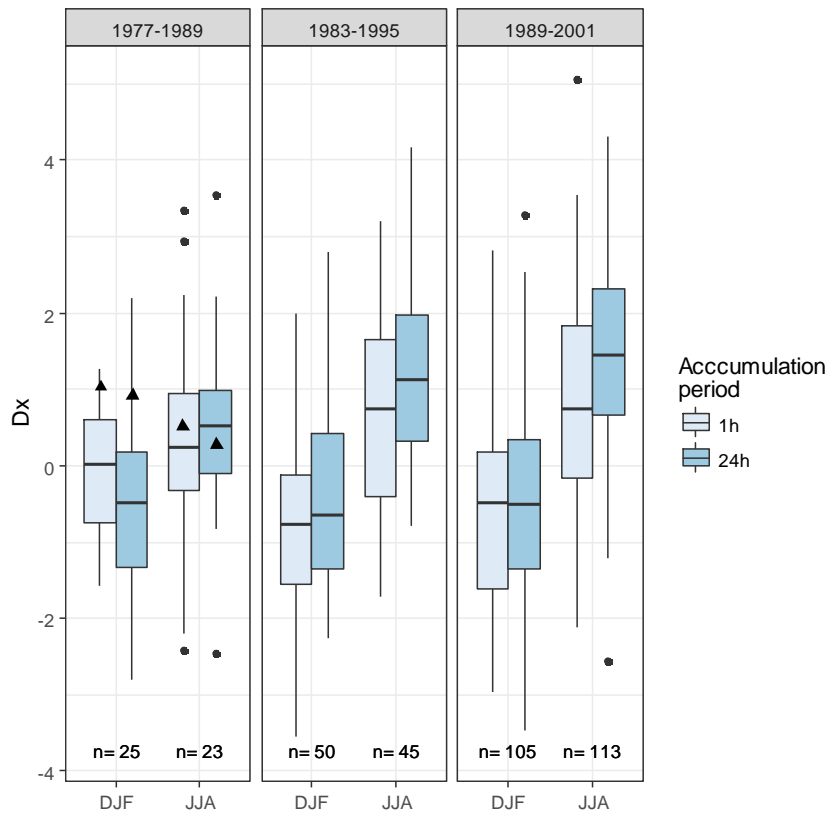
1102

1103



1104

1105 Figure 3: Percentage change in heavy rainfall intensity ( $\Delta p_{95}$ ) for the period 2002-2014 relative  
 1106 to successive rolling 13-year periods in the observations (top row 1h, middle row  
 1107 24h). Change is plotted at the midpoint of the earlier 13-year period. The solid line  
 1108 denotes the median of the change across all available gauges, the shading denotes the  
 1109 range bounded by the 10<sup>th</sup> and 90<sup>th</sup> percentile ranges where at least 15 gauges are  
 1110 available. The horizontal lines indicate the periods used to resample the observed  
 1111 time series to evaluate normalised change. The bar plots (bottom row) denote the  
 1112 number of gauges available for each period.



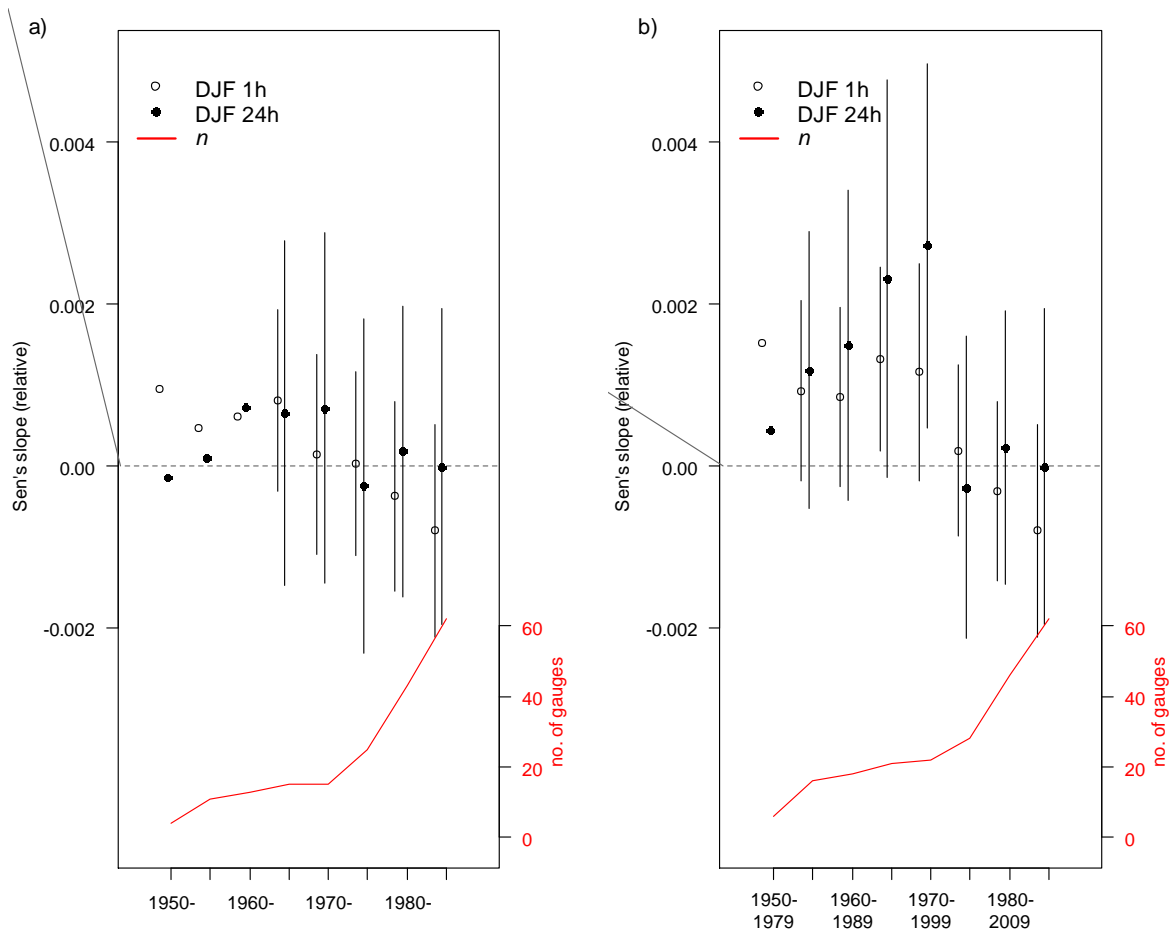
1113

1114

1115 Figure 4: Distribution of normalised change in heavy rainfall intensity ( $p_{95}, D_x$ ) for 1h and 24h  
 1116 accumulations for the period 2002-2014 relative to three 13 year periods in the  
 1117 observations. The black triangles denote the median of the corresponding 1.5km model  
 1118 results for a 25-year change (scaled linearly from the 100-year change). The value  $n$  denotes  
 1119 the number of gauges available for each period used to calculate change.

1120

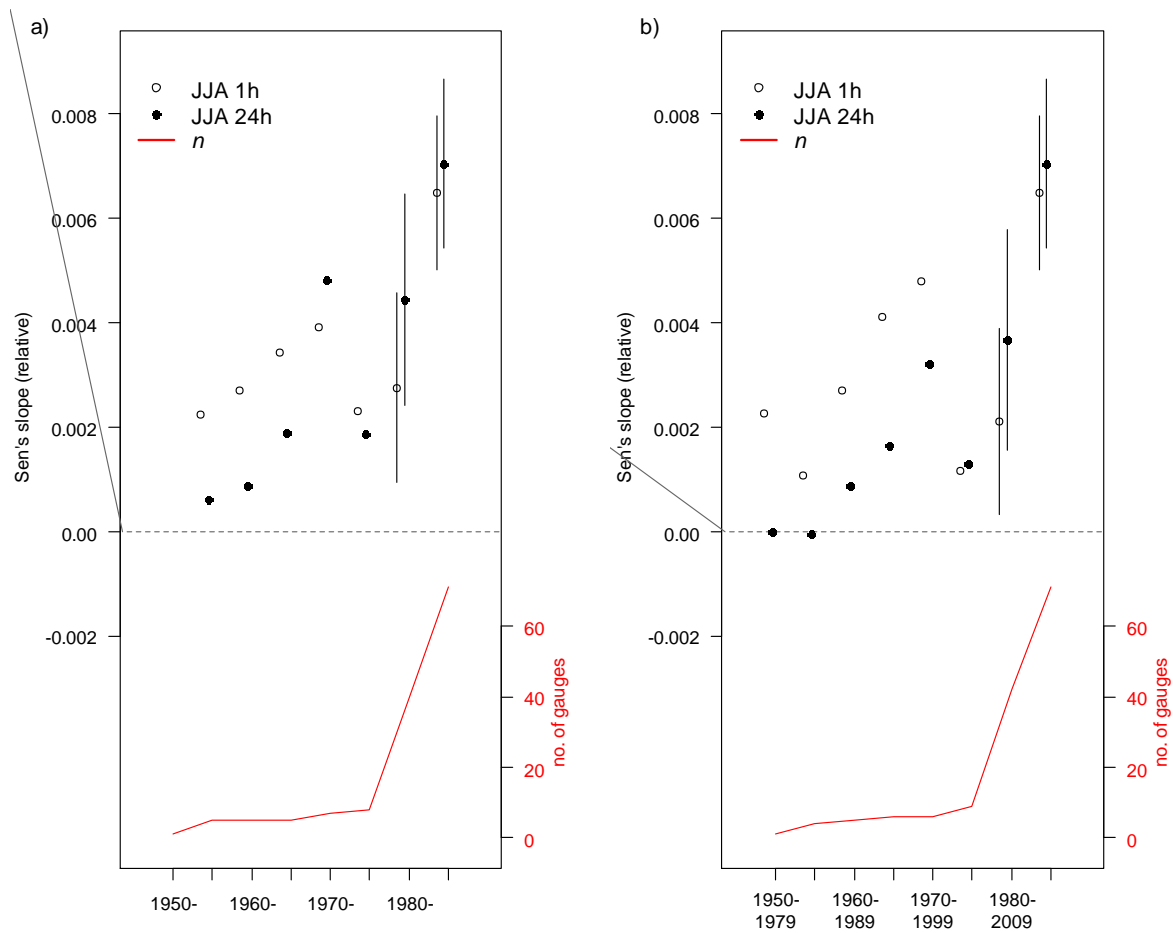
1121



1123

1124 Figure 5: Relative Sen's slope (unitless) for winter (DJF) hourly and daily heavy rainfall  
 1125 intensity ( $p_{95}$ ) in the observations for a) successive periods ending in 2014 (long  
 1126 trends) and b) successive 30y periods (running trends). Points show mean slope of  
 1127 all gauges whilst ranges show the 95% confidence interval estimated using the  
 1128 Student's t distribution when the number of gauges  $n \geq 15$  (see Supporting  
 1129 Information for method details). Lower plots shows the number of gauges used for  
 1130 each period.

1131

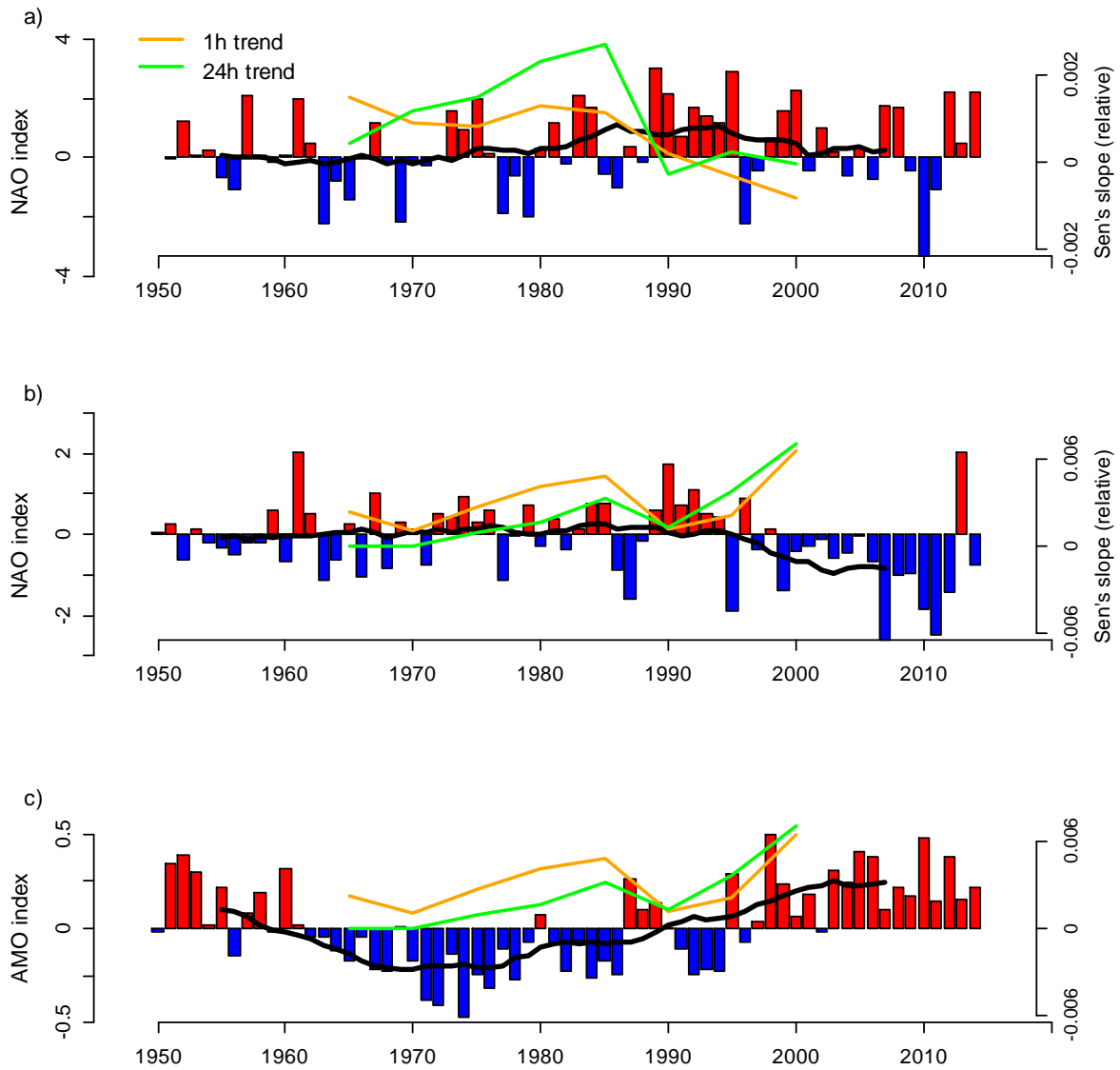


1132

1133 Figure 6: As in Figure 5 but for summer (JJA) hourly and daily heavy rainfall intensity ( $p_{95}$ ) in  
 1134 the observations.

1135





1136

1137 Figure 7: Time series of teleconnection indices for a) DJF NAO, b) JJA NAO, c) JJA AMO.

1138 The black line denotes the 15-year moving average. The orange and green lines indicate the

1139 mean seasonal relative Sen's slope for 1h and 24h  $p_{95}$  using running trends for each 30-year

1140 period plotted at the mid-year.

1141

1142 **Supporting Information**

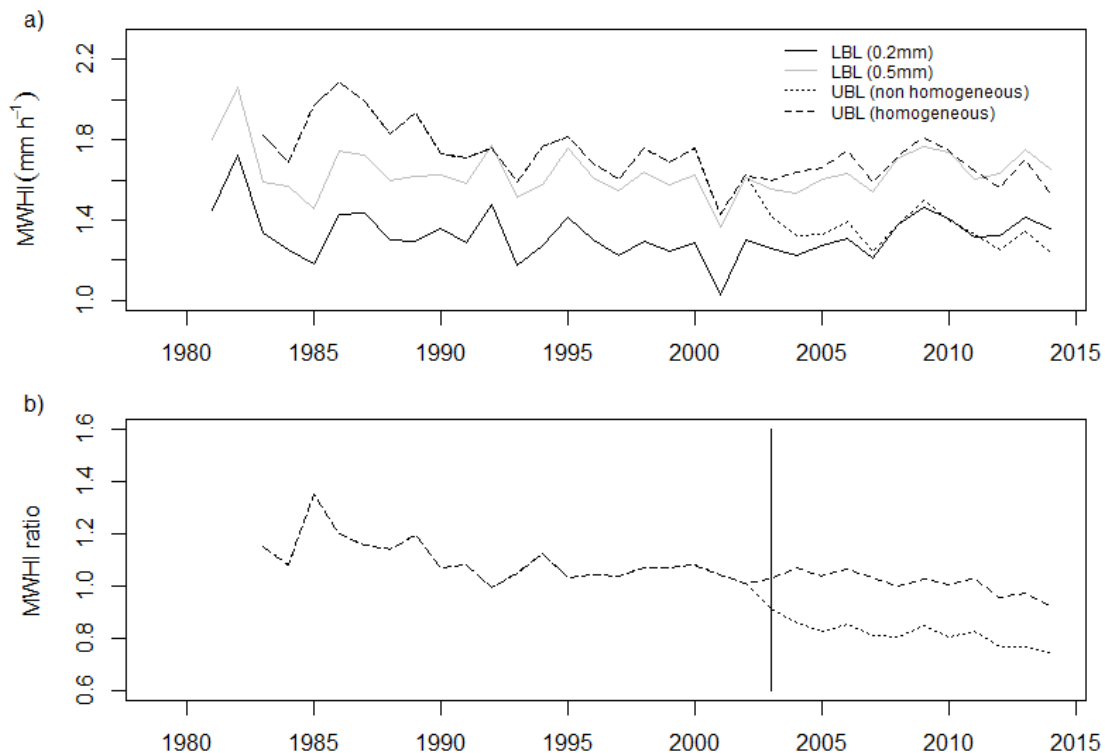
1143

1144 *Observed data homogeneity*

1145 Assessment of trends in time series may be confounded by inhomogeneities due to changes in the  
1146 observing system (e.g. appearing as abrupt discontinuities or gradual changes). Abrupt discontinuities  
1147 may occur due to changes in gauge relocation, instrumentation or observing and recording practices,  
1148 whilst gradual changes may be a consequence of a change in gauge surroundings or in the properties of  
1149 rain gauge characteristics (WMO, 2008). Several statistical tests are available to identify such  
1150 discontinuities. Here we apply three such tests, the Buishand range test (Buishand, 1982), Pettitt test  
1151 (Pettitt, 1979) and Standard Norman Homogeneity test (Alexandersson, 1986). We consider that a  
1152 series has a potential break in where at least two tests identify a significant break where the estimated  
1153 year of breaks are within 5 years of each other. Aguilar et al. (2003) recommend that homogeneity tests  
1154 are best performed on a time series that is expressed relative to a reference time series, i.e. one  
1155 experiencing the broad climatic influences of the candidate gauge (the gauge to be tested for  
1156 inhomogeneity). They suggest that inhomogeneities may be detected by comparing time series of the  
1157 ratios (in the case of precipitation) or differences (for temperature) as these should show neither sudden  
1158 changes, nor trends, which may be identified in a number of ways e.g. inspection of time series plots or  
1159 implementation of a statistical break point test. The above tests were therefore applied to annual time  
1160 series of gauge mean wet hour intensity (MWHI) expressed relative to a neighbouring gauge but only  
1161 where such gauges were located no more than 25km from the candidate gauge as Blenkinsop et al.  
1162 (2017) demonstrated a low correlation between gauges at greater distances, particularly in summer. As  
1163 some gauges did not have any qualifying neighbouring gauges these tests were therefore also applied  
1164 to annual time series of the absolute MWHI for each gauge.

1165 The application of these tests enabled the identification of a change in resolution of some tipping bucket  
1166 raingauge (TBR) measurements but due to the lack of gauge metadata (e.g. information on gauge  
1167 relocation or instrument changes) it was not possible to assess other potential causes. For example,  
1168 detected change points for the gauge at Upper Black Laggan (UBL), NW Scotland, matched a change  
1169 in measurement resolution from 0.5mm to 0.2mm in 2003 which accounted for a decrease in mean wet  
1170 hour intensity. As such changes in the resolution of measurement could affect trend analyses we  
1171 corrected changes in the precision of precipitation measurement through time following Groisman et  
1172 al. (2012), converting the finer-resolution measurements to the most coarse measurement for each gauge  
1173 throughout the entire period of record. Under this method, small precipitation amounts are gradually  
1174 accumulated until they reach the coarse resolution for each gauge. The effect of effect the change in  
1175 tip resolution and subsequent homogenisation on mean wet hour intensity is illustrated in Figure S1  
1176 which shows the (MWHI) for the gauge at UBL which is contrasted with a neighbouring gauge located  
1177 ~2km away. This indicates the reduction in mean intensities at UBL when the tip resolution increases

1178 from 0.5mm to 0.2mm resulting in a Sen's statistic (i.e. trend) of -0.023, significant at the 0.01 level  
 1179 (panel a). After homogenisation to a consistent resolution of 0.5mm Sen's statistics is lower (-0.008),  
 1180 still significant at the 1% level. The influence of tip resolution is further demonstrated by comparing  
 1181 the original time series for Lower Black Laggan (LBL; homogeneous at 0.2mm resolution) with the  
 1182 higher intensities when converted to the coarser resolution as the same total rainfall is distributed over  
 1183 fewer wet hours. In this instance, statistical tests did not identify a break point in the original time series  
 1184 but all three detected a break point at the year 2000 when the UBL time series is expressed relative to  
 1185 that of LBL (Figure S1b). Note that the break point detection time is not expected to exactly match that  
 1186 of a known homogeneity given noise in the time series but here the two are broadly consistent.  
 1187 Most gauges contained changes in gauge resolution (mainly 0.5mm to 0.2mm or 0.1mm to 0.2mm)  
 1188 although not all of these produced significant change points but were identified by changes in the time  
 1189 series of minimum non-zero rainfall amounts. A small number of gauges were considered unreliable  
 1190 and excluded on the basis of having more than one change in tip resolution. After homogenisation  
 1191 gauges were individually consistent at either 0.1mm, 0.2mm, 0.4mm or 0.5mm.  
 1192



1193  
 1194 Figure S1: Time series of a) annual mean wet hour intensity (MWHI) for gauges at Lower (LBL) and  
 1195 Upper Black Laggan (UBL), and b) the ratio between the annual values at the two locations  
 1196 (UBL/LBL). Data in a) for LBL are shown using tip resolution of 0.2mm and coarsened to  
 1197 0.5mm, and for UBL before and after homogenisation at the 0.5mm resolution. The ratio in  
 1198 b) is calculated using LBL at a resolution of 0.5mm. The vertical line denotes the timing of  
 1199 the change in tip resolution at UBL.

1200

1201 *Results from observed change analysis*

1202

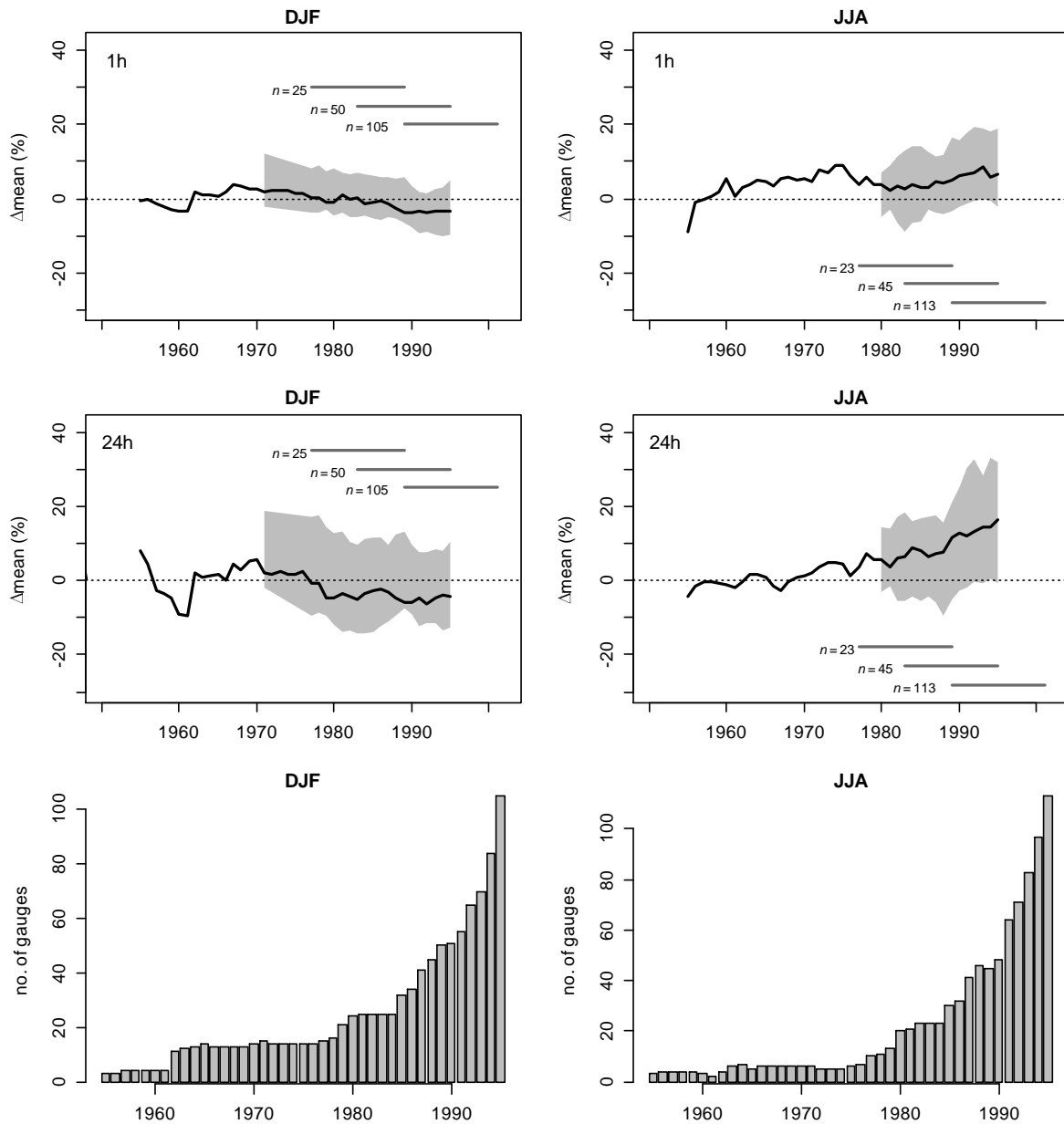
1203 Additional results supporting the main text and referred to therein are provided below. The confidence  
1204 intervals (CI) for the trend estimations in Figures 5 and 6 and Figures S5 and S10 are calculated using  
1205 the Student's t distribution where:

1206

1207 
$$CI = \bar{x} \pm t_{\alpha/2,df} \cdot \frac{s}{\sqrt{n}}$$

1208 where  $\bar{x}$  is the sample mean and  $t_{\alpha/2,df}$  is the t value associated with the required confidence level and  
1209 sample size. The sample standard deviation is denoted by  $s$ , and the sample size by  $n$ .

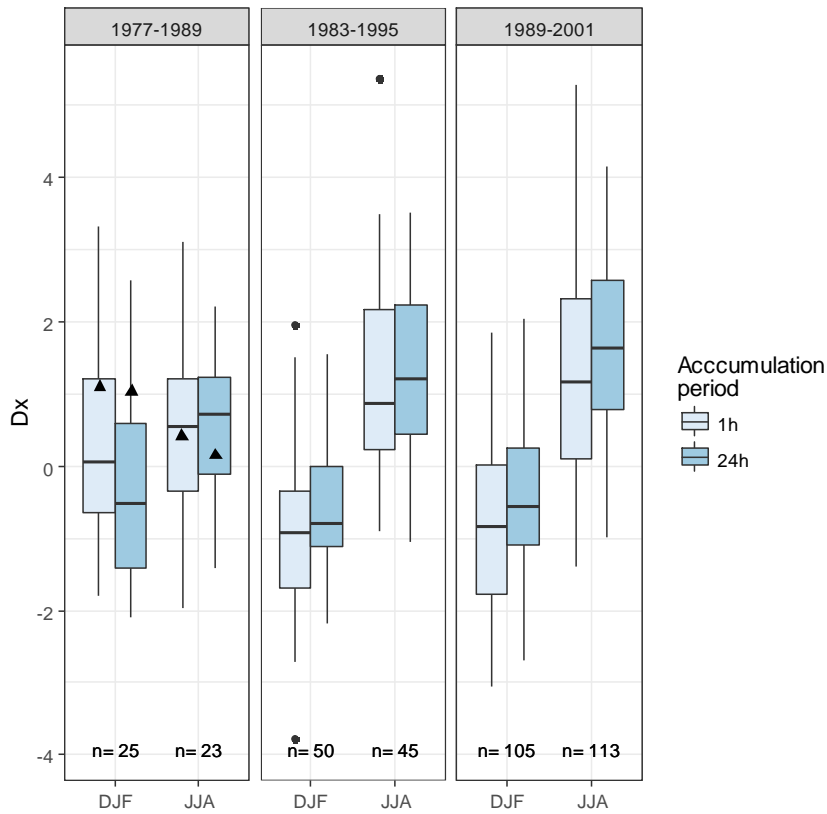
1210



1212

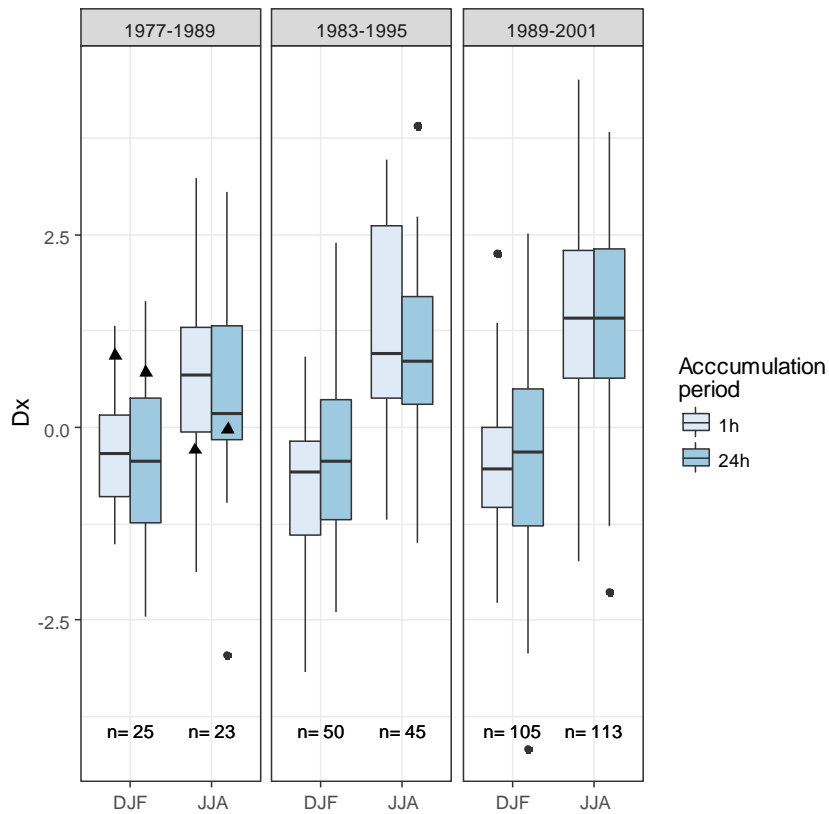
1213 Figure S2: Percentage change in mean precipitation intensity ( $\Delta\text{mean}$ ) for the period 2002-2014 relative  
 1214 to successive rolling 13-year periods in the observations (top row 1h, middle row 24h).  
 1215 Change is plotted at the midpoint of the earlier 13-year period. The solid line denotes the  
 1216 median of the change across all available gauges, the shading denotes the range bounded by  
 1217 the 10<sup>th</sup> and 90<sup>th</sup> percentile ranges where at least 15 gauges are available. The horizontal  
 1218 lines indicate the periods used to resample the observed time series to evaluate normalised  
 1219 change. The bar plots (bottom row) denote the number of gauges available for each period.  
 1220

1221



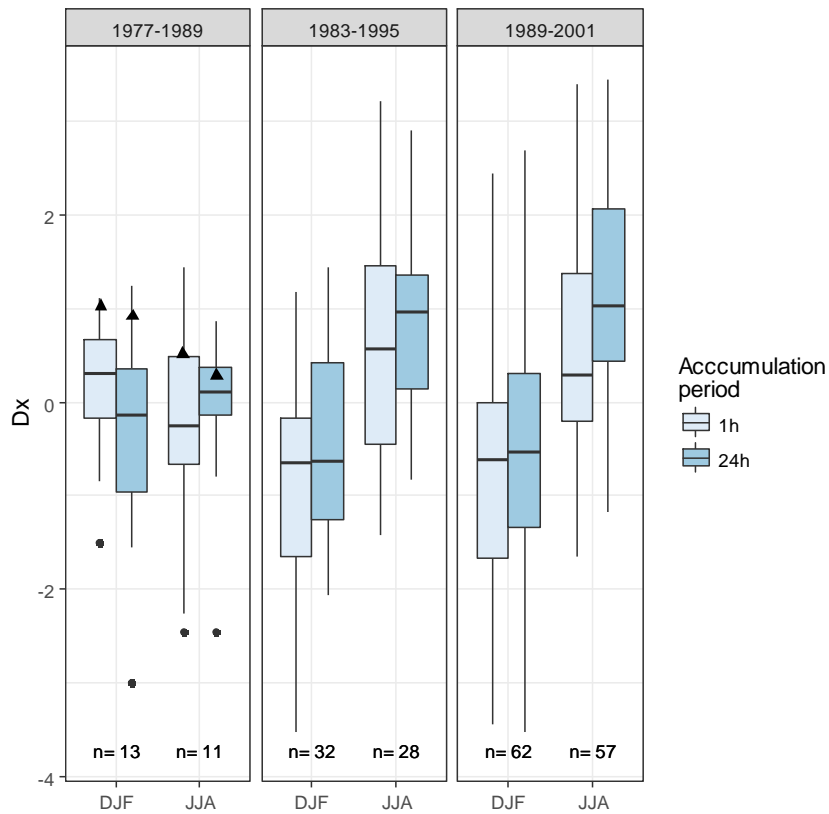
1222

1223 Figure S3: Distribution of normalised change in mean precipitation intensity (mean,  $D_x$ ) for 1h and 24h  
1224 accumulations for the period 2002-2014 relative to three 13-year periods in the  
1225 observations. The black triangles denote the median of the corresponding 1.5km model  
1226 results for a 25-year change (scaled linearly from the 100-year change). The value  $n$   
1227 denotes the number of gauges available for each period used to calculate change.  
1228



1229  
 1230  
 1231  
 1232  
 1233  
 1234  
 1235

Figure S4: Distribution of normalised change in heavy precipitation ( $p_{99ALL}, D_x$ ) for 1h and 24h accumulations for the period 2002-2014 relative to three 13-year periods in the observations. The black triangles denote the median of the corresponding 1.5km model results for a 25-year change (scaled linearly from the 100-year change). The value  $n$  denotes the number of gauges available for each period used to calculate change.



1236

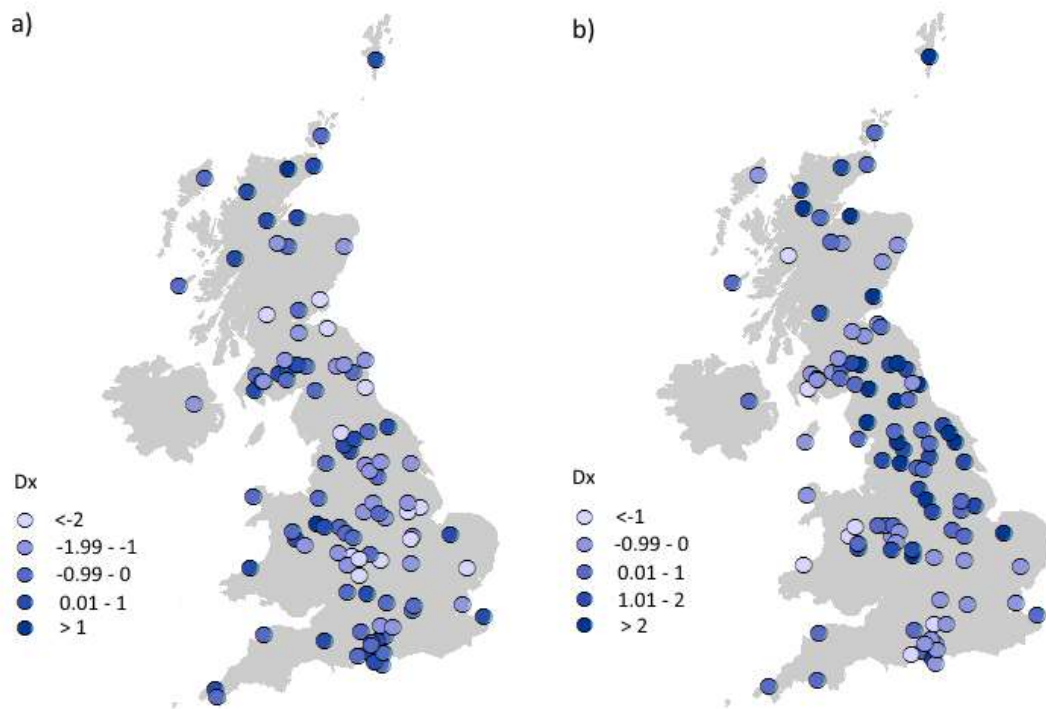
1237

1238 Figure S5: Distribution of normalised change in heavy precipitation intensity ( $p_{95}, D_x$ ) for 1h and 24h  
 1239 accumulations for the period 2002-2014 relative to three 13-year periods in the observations.  
 1240 Here, only those gauges in the climate model domain (southern UK, see Figure 1) are used.  
 1241 The black triangles denote the median of the corresponding 1.5km model results for a 25-  
 1242 year change (scaled linearly from the 100-year change). The value  $n$  denotes the number of  
 1243 gauges available for each period used to calculate change.

1244

1245



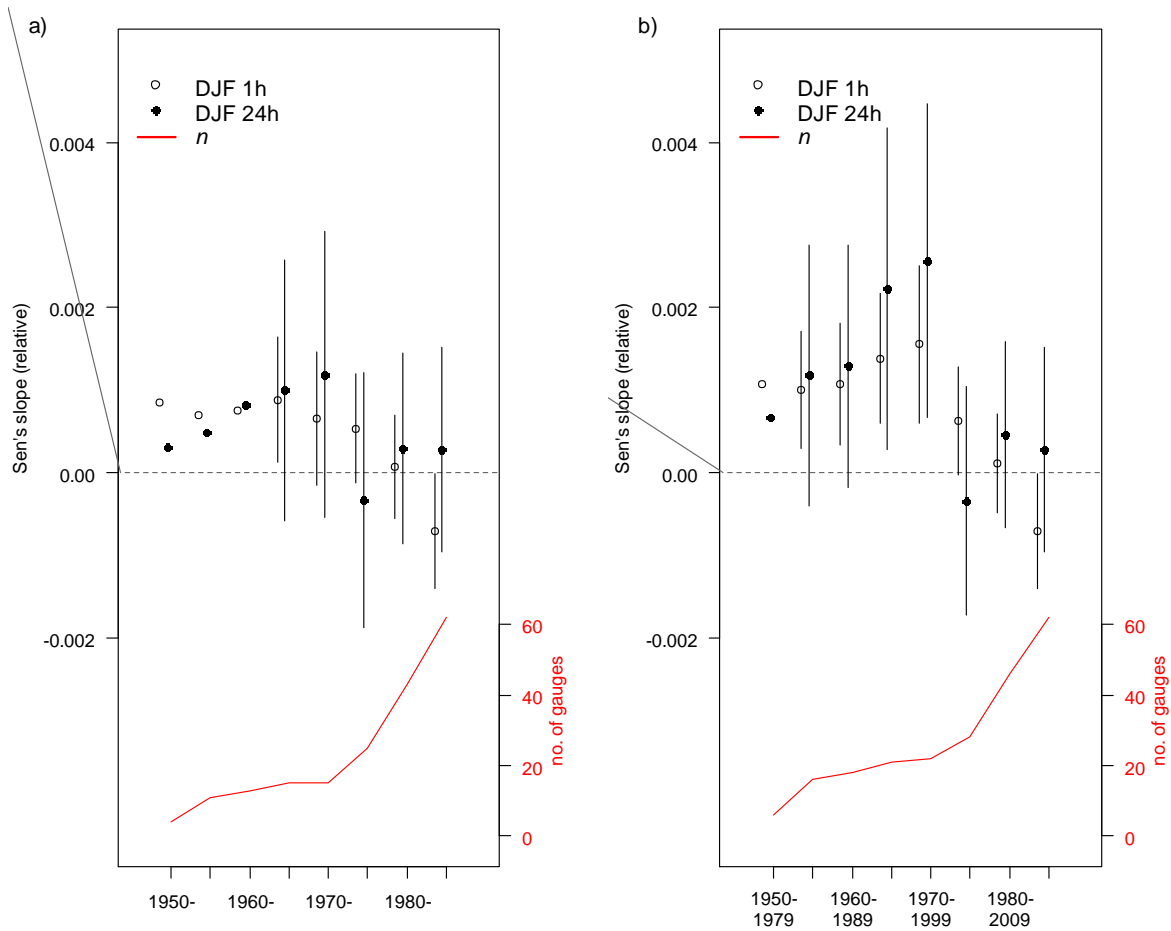


1246

1247 Figure S6: Spatial distribution of normalised change in heavy precipitation intensity ( $p_{95}, D_x$ ) for 1h  
 1248 accumulations for the period 2002-2014 relative to 1989-2001 for a) DJF and b) JJA.

1249

1250



1251

1252

1253

1254

1255

1256

1257

1258

1259

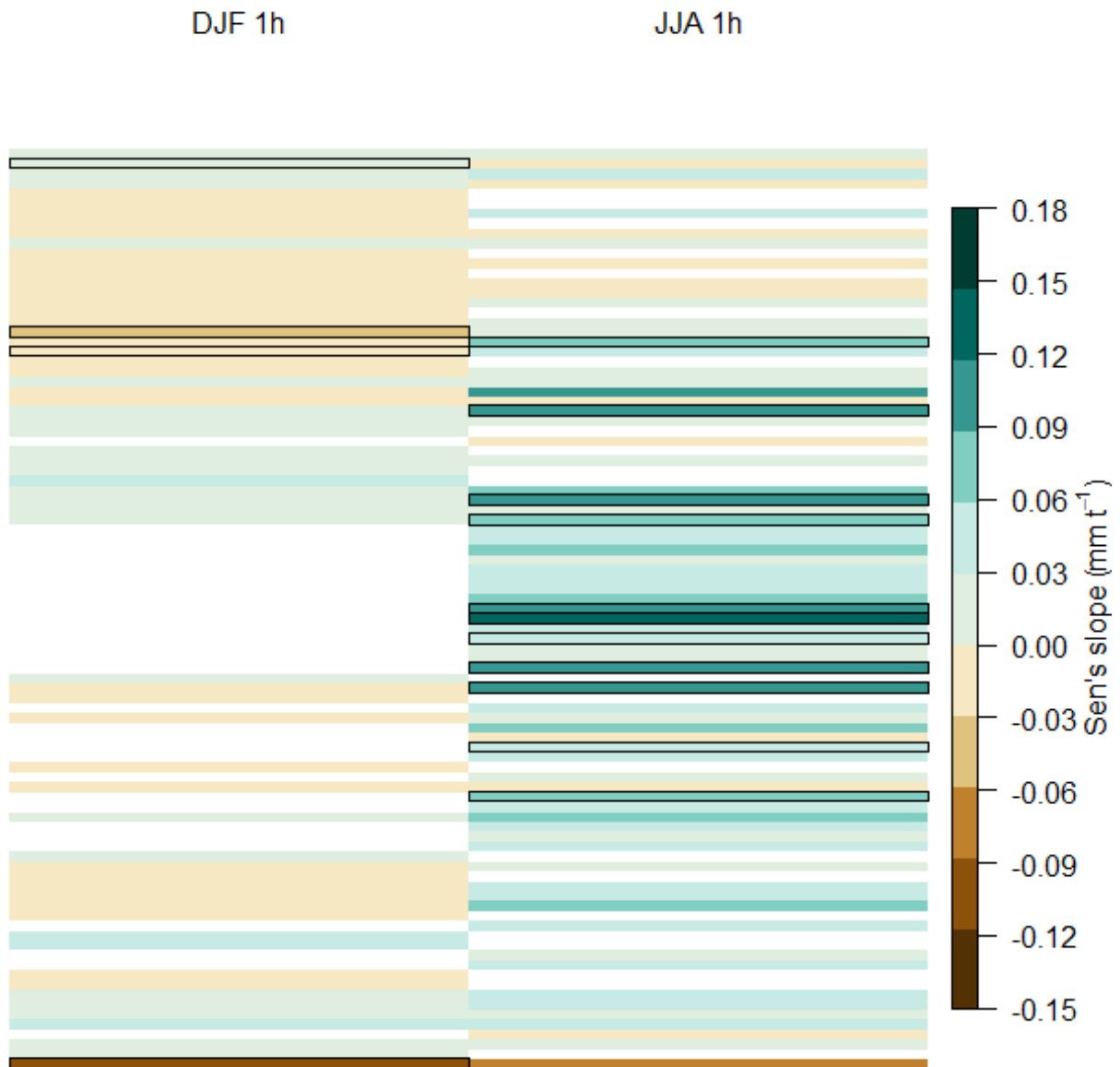
1260

1261

1262

1263

Figure S7: Relative Sen's slope (unitless) for winter (DJF) hourly and daily mean rainfall intensity for a) successive periods ending in 2014 (long trends) and b) successive 30y periods (running trends). Points show mean slope of all gauges whilst ranges show the 95% confidence interval estimated using the Student's t distribution when the number of gauges  $n \geq 15$ . Lower plots shows the number of gauges used for each period. See main paper for a description of the relative Sen's slope.



1264

1265

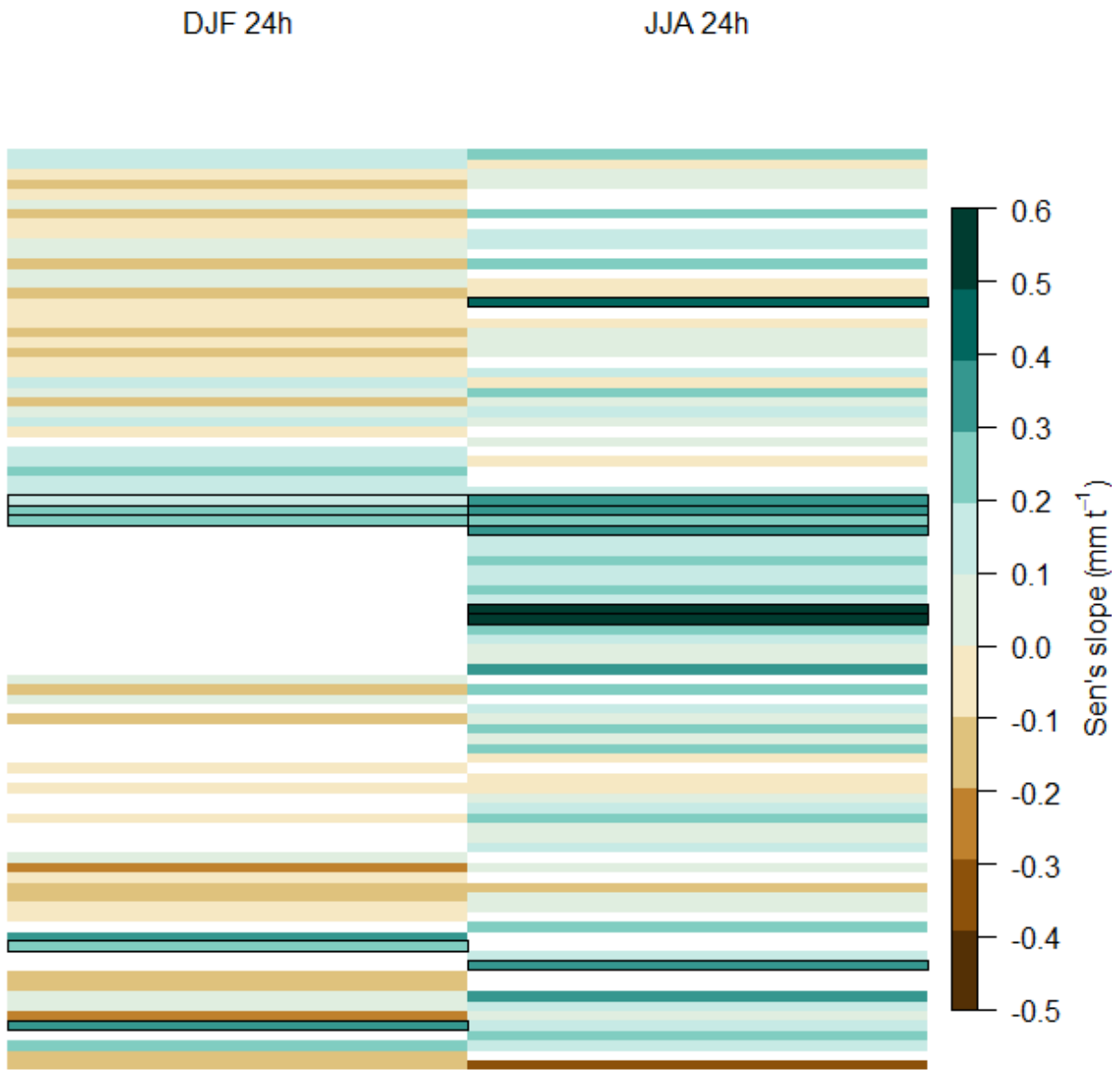
1266

1267

1268

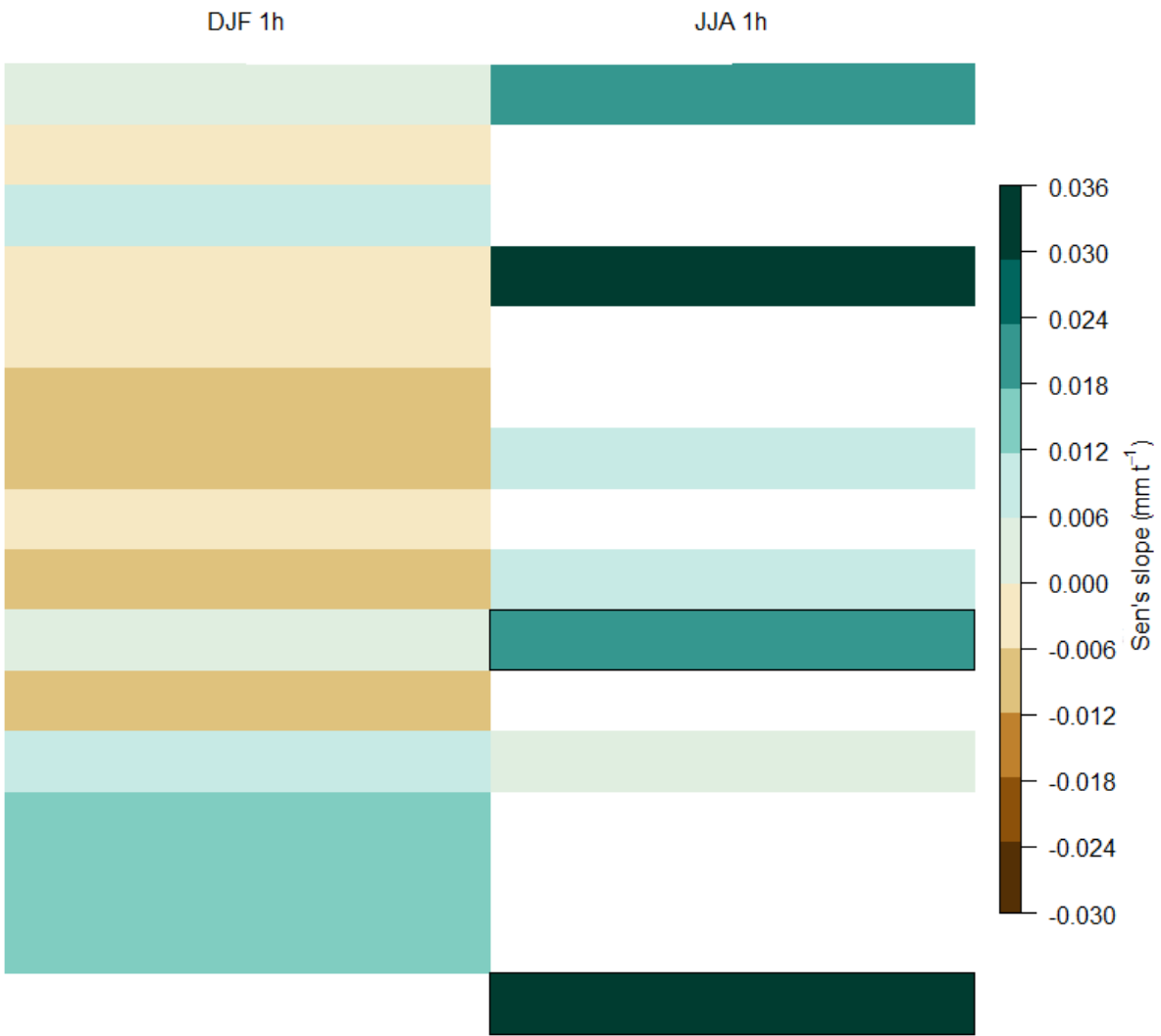
1269

Figure S8: Sen's slope statistics (absolute) for 1h  $p_{95}$  for the period 1985-2014. Each row represents a different gauge, outlined boxes denote significance at the 95% level using the Mann-Kendall test. White areas denote gauges that do not meet completeness criteria for that season.



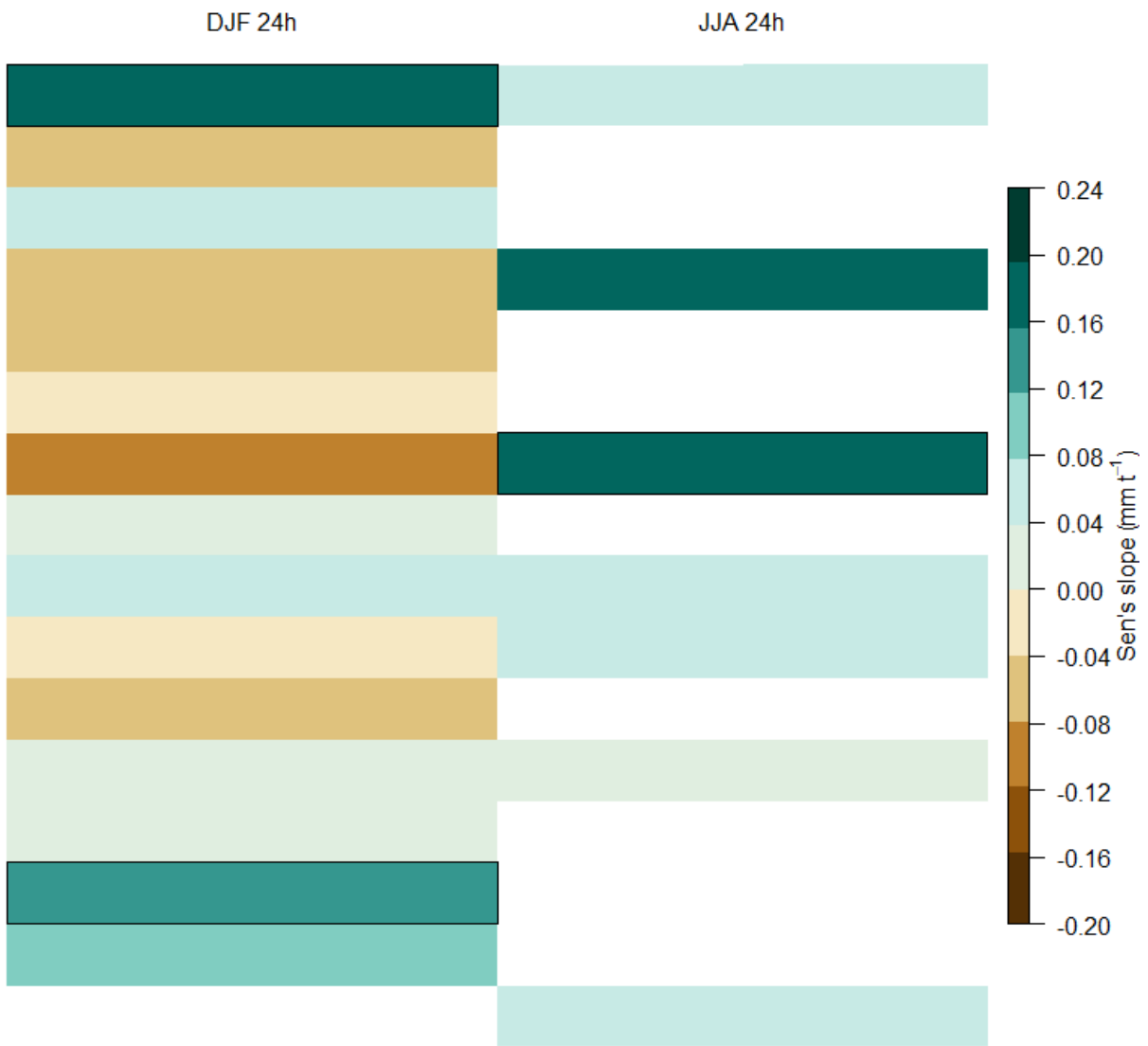
1270

1271 Figure S9: As in Figure S8 but for 24h  $p_{95}$ .



1272  
 1273  
 1274  
 1275  
 1276  
 1277  
 1278

Figure S10: Sen's slope statistics for 1h  $p_{95}$  for the period 1970-2014. Each row represents a different gauge, outlined boxes denote significance at the 95% level using the Mann-Kendall test. White areas denote gauges that do not meet completeness criteria for that season.



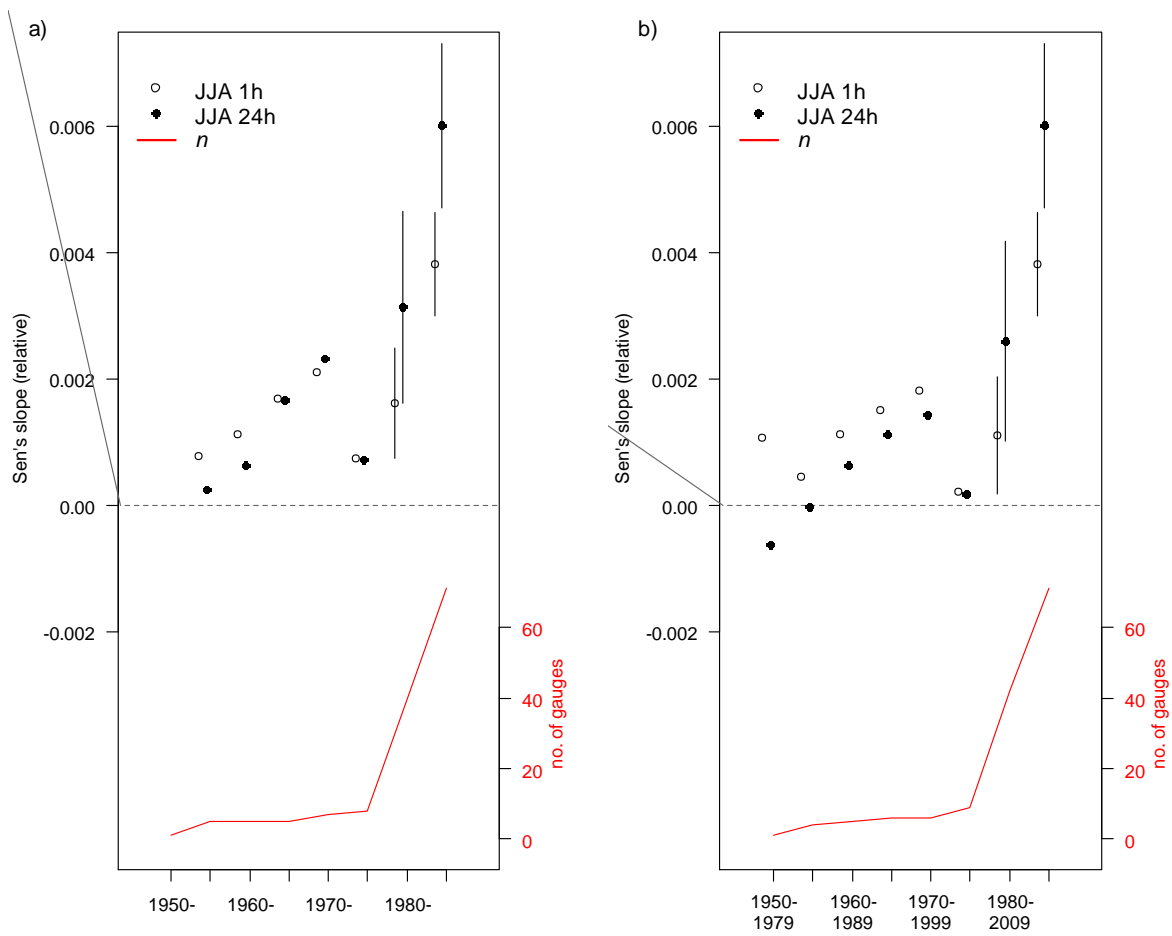
1279

1280 Figure S11: As in Figure S10 but for 24h  $p_{95}$ .

1281

1282

1283

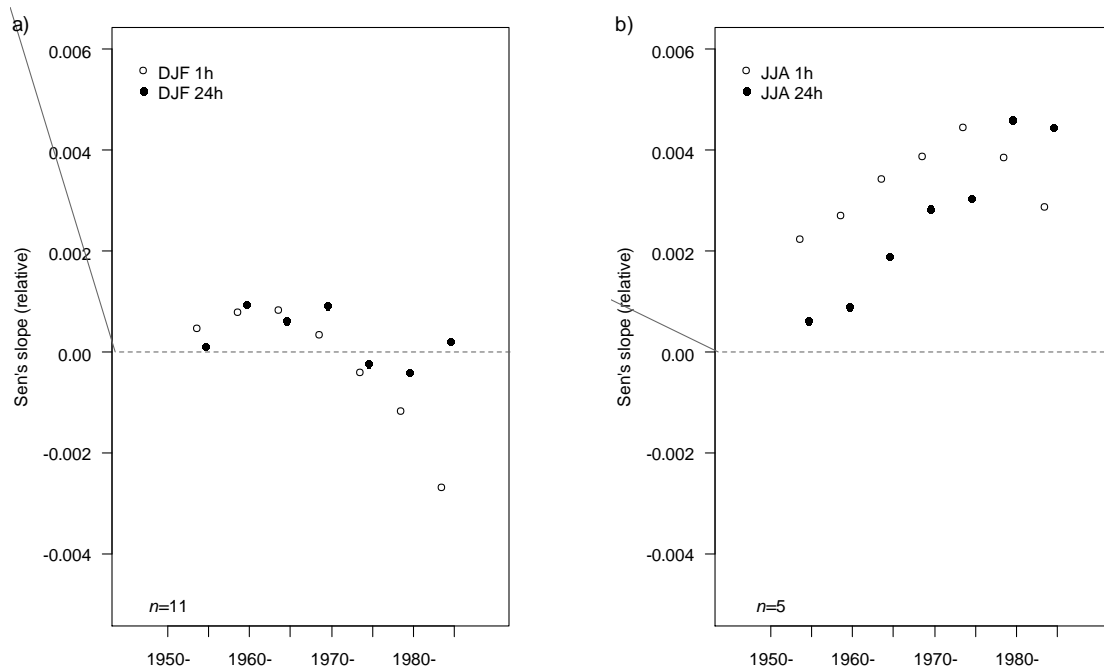


1284

1285 Figure S12: As in Figure S7 but for summer (JJA) hourly and daily mean rainfall intensity.

1286

1287



1288

1289

1290 Figure S13: Relative Sen's slope (unitless) for a) winter (DJF) and b) summer (JJA) hourly and daily  
 1291 heavy precipitation intensity ( $p_{95}$ ) for successive periods ending in 2014 (long trends).  
 1292 Points show mean slope using only those gauges for which trends may be calculated for  
 1293 all periods from 1955,  $n$  denotes the number of gauges. See main paper for a description  
 1294 of the relative Sen's slope.

1295

1296

1297 *Variance estimates from model and observations*

1298

1299 Variance in 13-year heavy precipitation intensity ( $p_{95}$ ) obtained by bootstrap resampling the 13 years  
 1300 of data in the control (future) period  $\sigma_c^2$  ( $\sigma_f^2$ ) for the model are shown below in Tables S1 and S2.  
 1301 Also shown are variance estimates for the observations, for the 2002-2014 period, again estimated by  
 1302 bootstrap resampling the 13 years of data. It can be seen that the variance estimates agree well  
 1303 between the observations and the model control simulation, for precipitation accumulated on both the  
 1304 daily and hourly timescale, which gives credibility to the noise estimation that goes into the model  
 1305 detection time estimates.

1306



	<b>1.5km</b>	<b>5km</b>	<b>12km</b>	<b>50km</b>
<b>Daily (Control)</b>	<b>1.676</b> <b>(0.700,4.449)</b>	<b>1.662</b> <b>(0.693,4.235)</b>	<b>1.461</b> <b>(0.621,3.842)</b>	<b>1.060</b> <b>(0.558,2.575)</b>
<b>Daily (Future)</b>	<b>6.647</b> <b>(2.620,21.115)</b>	<b>6.697</b> <b>(2.532,20.740)</b>	<b>5.957</b> <b>(2.567,19.000)</b>	<b>4.984</b> <b>(2.229,16.218)</b>
<b>Hrly (Control)</b>	<b>0.038</b> <b>(0.018,0.085)</b>	<b>0.035</b> <b>(0.016,0.078)</b>	<b>0.028</b> <b>(0.013,0.065)</b>	<b>0.016</b> <b>(0.009,0.030)</b>
<b>Hrly (Future)</b>	<b>0.088</b> <b>(0.036,0.258)</b>	<b>0.082</b> <b>(0.034,0.236)</b>	<b>0.072</b> <b>(0.028,0.196)</b>	<b>0.048</b> <b>(0.016,0.107)</b>
<b>Daily (Observations)</b>	<b>1.554</b> <b>(0.663,4.130)</b>	-	-	-
<b>Hrly (Observations)</b>	<b>0.043</b> <b>(0.020,0.095)</b>	-	-	-

1308

1309

1310 Table S1: Variance in 13-year heavy precipitation intensity ( $p_{95}$ ) in winter ( $\text{mm}^2$ ), for the control (blue)  
 1311 and future (red) periods, for precipitation accumulated across a range of space (1.5km-50km)  
 1312 and time (hrly-daily) scales. Comparable results are shown for observations (green) calculated  
 1313 over the period 2002-2014 but at the point scale. Shown is the median of the variance across  
 1314 southern UK land points, and in brackets are the 10th and 90th percentiles of the spatially  
 1315 varying variance estimates. Variance is calculated across 100 estimates of  $p_{95}$  obtained by  
 1316 bootstrap resampling the observed or model simulated precipitation time series.

1317

1318

	<b>1.5km</b>	<b>5km</b>	<b>12km</b>	<b>50km</b>
<b>Daily (control)</b>	<b>8.337</b> (3.577,22.997)	<b>7.823</b> (3.313,22.310)	<b>6.883</b> (3.008,21.842)	<b>4.814</b> (2.138,11.778)
<b>Daily (future)</b>	<b>24.245</b> (8.799,63.433)	<b>21.355</b> (7.951,56.065)	<b>18.272</b> (7.121,47.927)	<b>11.051</b> (3.887,33.724)
<b>Hrly (control)</b>	<b>0.364</b> (0.162,0.791)	<b>0.301</b> (0.131,0.663)	<b>0.220</b> (0.091,0.512)	<b>0.095</b> (0.041,0.212)
<b>Hrly (future)</b>	<b>1.528</b> (0.588,3.854)	<b>1.090</b> (0.443,2.601)	<b>0.665</b> (0.277,1.468)	<b>0.210</b> (0.082,0.499)
<b>10min (control)</b>	<b>0.040</b> (0.019,0.083)	<b>0.028</b> (0.013,0.056)	<b>0.018</b> (0.007,0.037)	<b>0.008</b> (0.003,0.019)
<b>10min (future)</b>	<b>0.172</b> (0.071,0.444)	<b>0.093</b> (0.042,0.219)	<b>0.046</b> (0.020,0.115)	<b>0.013</b> (0.005,0.039)
<b>Daily (Observations)</b>	<b>5.454</b> (2.539,13.444)	-	-	-
<b>Hrly (Observations)</b>	<b>0.244</b> (0.108,0.655)	-	-	-

1319

1320

1321

Table S2: As Table S1 but for variance in 13-year heavy precipitation intensity ( $p_{95}$ ) in summer ( $\text{mm}^2$ ).

1322 **References**

- 1323 Aguilar E, Auer I, Brunet M, Peterson TC, Wieringa J, 2003. Guidance on metadata and  
1324 homogenization. WMO TD N. 1186 (WCDMP N. 53); 51pp.
- 1325 Alexandersson H, 1986. A homogeneity test applied to precipitation data. *International Journal of*  
1326 *Climatology*, 6, 661-675.
- 1327 Blenkinsop S, Lewis E, Chan SC, Fowler HJ, 2017. An hourly precipitation dataset and climatology  
1328 of extremes for the UK. *International Journal of Climatology*, **37**, 722–740.
- 1329 Buishand TA, 1982. Some methods for testing the homogeneity of rainfall records. KNMI Scientific  
1330 Report WR 81-7, De Bilt, The Netherlands.
- 1331 Groisman PY, Knight RW, Karl TR, 2012. Changes in intense precipitation over the central United  
1332 States, *J. Hydrometeorol.*, **13**, 47–66. doi:10.1175/JHM-D-11-039.1.
- 1333 Pettitt AN, 1979. A non-parametric approach to the change-point detection. *Applied Statistics*, 28,  
1334 126-135.
- 1335 WMO, 2008. Guide to Meteorological Instruments and Methods of Observation, WMO-No. 8, Geneva,  
1336 Switzerland.
- 1337
- 1338